
Article:
Whalley, W.B. orcid.org/0000-0003-3361-3527 (2023) Glacier–rock glacier interactions in the eastern Hindu Kush, Nuristan, Afghanistan [35.92,71.13] in the period 1976–2019. Geografiska Annaler: Series A, Physical Geography, 105 (2-3). pp. 91-120. ISSN: 0435-3676

https://doi.org/10.1080/04353676.2024.2321425

Taylor & Francis
Taylor & Francis Group

GEOGRAFISKA ANNALER SERIES A PHYSICAL GEOGRAPHY

Geografiska Annaler: Series A, Physical Geography

ISSN: 0435-3676 (Print) 1468-0459 (Online) Journal homepage: www.tandfonline.com/journals/tgaa20

Glacier–rock glacier interactions in the eastern Hindu Kush, Nuristan, Afghanistan [35.92,71.13] in the period 1976–2019

W. Brian Whalley

To cite this article: W. Brian Whalley (2023) Glacier–rock glacier interactions in the eastern Hindu Kush, Nuristan, Afghanistan [35.92,71.13] in the period 1976–2019, Geografiska Annaler: Series A, Physical Geography, 105:2-3, 91-120, DOI: 10.1080/04353676.2024.2321425

To link to this article: https://doi.org/10.1080/04353676.2024.2321425

Published online: 27 Mar 2024.

GEOGRAFISKA ANNALER: SERIES A, PHYSICAL GEOGRAPHY
2023, VOL. 105, NOS. 2–3, 91–120
https://doi.org/10.1080/04353676.2024.2321425

Glacier–rock glacier interactions in the eastern Hindu Kush, Nuristan, Afghanistan [35.92,71.13] in the period 1976–2019

W. Brian Whalley

Department of Geography, University of Sheffield, Sheffield, UK

ABSTRACT

Landsystem relationships between glaciers and rock debris supply in a mountain landscape domain, (𝔻𝕞), are described. Decimal latitude-longitude [dLL] geolocations are used to identify features and transects in an information landscape. Geo-located features are coded, enabling transects between a 1976 expedition and 2019 Google Earth imagery to be compared. Rock debris is progressively added to 1-3 km long glaciers which become debris-covered. Cirque glaciers eventually assume rock glacier (**RG**) forms when supraglacial debris loads are high. Some rock glacier snouts reach main valley floors and still advance over meadows. This behaviour is attributed to high geomorphic activity producing rock detritus and transport to glaciers in the early Little Ice Age. The advances of rock glacier snouts are a consequence of thinning; low-angle glaciers still moving beneath debris-covered glaciers (**GLd**) covers. Persistent melt pools continue to develop within the surface debris cover of glaciers and rock glaciers and expose glacier ice. All the rock glaciers are below the regional snowline and permafrost can be discounted for rock glacier formation. Scree slope (**SS**) development may ultimately be sufficient to cover bare glacier ice moving from a glacier (**GL**) to debris-covered glacier (**GLd**) to rock glacier (**RG**). Reverse slopes in the debris at the foot of screes mark the mass continuum of glacier flow below the debris cover, not the 'rooting zone' of a permafrost-derived **RG**. Scree slopes themselves show no evidence of rock glacier-like flow. A simple glacier ice-debris transport continuum model is sufficient and necessary for rock glacier formation and flow.

ARTICLE HISTORY
Received 28 February 2023
Revised 22 November 2023
Accepted 17 February 2024

KEYWORDS
glacier; rock glacier; weathered debris supply; Little Ice Age; mountain landscape domain; information landscape

Introduction

This paper examines an area of glaciers and rock glaciers in the Hindu Kush (HK) in the light of field observations in 1976 and 2019 satellite imagery. I examine evidence for rock glaciers as being glacial (glacigenic) features and for evidence of 'permafrost rock glaciers'. A landsystem approach, using terrestrial and Google Earth imagery, is used to examine these notions and the 'geomorphological slope sequence' (RGIK 2022) to examine debris movement connectivity in a high mountain domain.

The significance of rock glaciers; whether they represent 'glacial' features or result from 'permafrost creep', has long been a contested issue (Martin and Whalley 1987; Whalley and Martin 1992).

CONTACT W. Brian Whalley b.whalley@sheffield.ac.uk Department of Geography, University of Sheffield, Sheffield, S3 7ND, UK

Barsch (1996), in an influential book, promoted the 'permafrost rock glacier', that is, rock glaciers are *only* the product of the creep of interstitial ice, accrued as permafrost, within a rocky rubble matrix. Despite evidence that many rock glaciers have demonstrable glacier ice cores, the 'glacial' model has been generally neglected. That glaciers *do* provide the basic core for rock glacier formation has a long observational pedigree, most notably Potter's (1972) work on Galena Creek Rock Glacier [L1], (the Location List at the end gives [dLL] locations not in the field area). Several papers in Geografiska Annaler (1998: Potter et al. (1998), Steig et al. (1998)) and Whalley (2023a) also refer to ice exposures at Galena Creek. Recent long-term studies using a landsystem approach show rock glacier development in the Alps (Whalley 2020, 2021a) [L2], Iceland (Whalley 2021b) [L3] and the Pyrenees (Whalley 2021c) [L4].

Evidence for glacigenic (i.e. glacier-derived) rock glaciers has been criticized by Barsch (1996, p. 215) concluding, after Wahrhaftig and Cox (1959), that 'it is difficult to escape the conclusion that the motion of rockglaciers is the motion of frozen rubble' (p. 215). The International Permafrost Association (IPA) aims to standardize rock glacier inventories; it defines (RGIK 2022, p. 6, emphasis added) rock glaciers as,

> *debris landforms generated by a former or current creep of frozen ground (permafrost), detectable in the landscape with the following morphologies: front, lateral margins and optionally ridge-and-furrow surface topography.* In a *geomorphological slope sequence*, rock glaciers are (or were) landforms conveying debris from an upslope area (source area or rooting zone) towards their front.

Rock glaciers have thus been used to map 'mountain permafrost', being 'an important component of high mountain systems, characteristically serving as a visible indicator of mountain permafrost' (Janke et al. 2013). The RGIK (2022) report defined permafrost with rock glacier types used by (Hu et al. 2023) who employed a 'deep learning' approach for mapping. In some areas, rock glaciers have been presumed to be indicators of permafrost where a 'permafrost favorability index' has been used to 'model accurately rock glacier distribution' (Marcer et al. 2017).

Bolch et al. (2019) indicated that, for the 'extended Hindu Kush Himalaya Region … Outside China, there has been no systematic collection of permafrost data in the extended HKH region to date, … systematic remote mapping of rock glaciers' (Schmid et al. 2015). Schmid et al. (2015) aimed to provide, 'a first-order assessment of these permafrost maps in the HKH region based on the mapping of rock glaciers'. Rock glaciers and glaciers have also been viewed in the context of water resources in the Himalaya (Jones et al. 2018; Vishwakarma et al. 2022) and more generally by Jones et al. (2019), where both 'glacial' and 'permafrost' models are considered. Chakravarti et al. (2022) considered the water storage aspect but also view rock glaciers as permafrost indicators (p. 226), linking to Schmid et al. (2015).

This paper examines the evidence in a high mountain domain in the Hindu Kush for:

(1) Glacier–debris-covered and glacier–rock glacier occurrences and possible transitions between.
(2) The existence of permafrost independently of the cryogenic RG model and using
(3) Landsystem approaches with mapped transects to identify material movement over time.

Methodology and methods

Schmid et al. (2015) used rock glaciers as a permafrost proxy, 'because they are *visual indicators of permafrost*, can occur near the *lowermost regional occurrence of permafrost in mountains*, and can be delineated based on high-resolution remote sensing imagery freely available on Google Earth' … 'We use the mapping of rock glaciers in Google Earth as *first-order evidence for permafrost* in mountain areas with *severely limited ground truth*'.

For identification: a

> Geomorphological approach: rock glaciers are recognized by a systematic visual inspection of the (imaged) landscape and DEM [digital elevation model] -derived products. … surface texture and morphometric analysis could also be used. This is the classical approach, locally complemented by field visits. It allows the production of exhaustive inventories of presumed moving and non-moving landforms, whose discrimination (activity classes) is primarily based on geomorphological characteristics. Development in deep-learning techniques could also complement this approach. (RGIK 2022, pp. 5–6)

The 'geomorphological approach' is used here by examining geomorphological characteristics and change over 40 years via landsystems. In 1976, no aerial photographs were available, but Google Earth (GE) examination is now possible at sufficient resolution for mapping, and here supplemented by 1976 images. Decimal latitude-longitude (dLL) location (Whalley 2021a, 2023a) allows precise feature identification and comparison with other sites. Points and transects are identified as [dLL] tuples; [dLat,dLong] with transects as [dLat,dLong],bearing in degrees. Locations in the HK study area have [dLL] in the text, comparison locations elsewhere are cited in the text, [L1 etc] and in a list towards the end of the paper. Identifying landforms as [dLL] allows data, particularly landform identification, to better conform to the FAIR principles; findability, accessibility, interoperability and reusability of data (Whalley 2023a).

Landsystem approach to geomorphological mapping in mountains

The concept of landsystems was popularized by Evans (2003) for glacial systems, 'the elements and units were placed in the context of glaciated basins'. The approach taken here is that *any* landform can be identified and mapped as a distinctive geo-located entity within any 'landscape domain' ($\mathbb{LD}$). The landsystem approach as used in this paper becomes part of Gore's Digital Earth project (Gore 1999). The recognition of 'periglacial' and 'paraglacial ' environments, terms that are not themselves significant, are misleading under changing environments but may be contained within a mountain domain $\mathbb{Dm}$, a landform/process subset of a more general $\mathbb{LD}$. The landsystem methodology (Whalley 2020, 2021a, 2021b) is used to identify sediment and snow/ice transfer paths in a high mountain area of Eastern Afghanistan. The system is the movement of material mass along potential energy gradients (usually downslope). Movement occurs according to the strength of the material and continuum mechanics as slope debris (or water or ice) respond to shear stresses via the appropriate constitutive equations. This paper maps features along stress gradients that show the movement of material over variable periods. Transects allow examination of system connectivity (McRae 2008) over time as well as comparisons between transects (Whalley 2022). Inputs and responses, such as magnitude/frequency of talus supply from and to landform elements, are generally not known in detail so we currently lack the information required to construct time-dependent (partial) differential equations to quantify such transfers. However, the landsystem approach allows initial investigation of time-integrated mechanisms producing landform changes, here 1976-2019. The geomorphic 'processes' are given by an 'operator' notation for simple material transport paths: dry+/-water movement $\rightarrow$, snow/ice movement $\dashrightarrow$. When $\dashrightarrow\!\!\rightarrow$ act together, slush/debris avalanches for example, the composite $\twoheadrightarrow$ is used. A hydrological operator, denoted by $\rightsquigarrow$, includes discharges, water chemistry etc. *In situ* weathering is denoted by $\downarrow$. In a mountain context, $\rightarrow$ might signify dry rockfall from a free face or as 'dry ravel'; 'a general term that describes the rolling, bouncing, and sliding of individual particles down a slope and is a dominant hillslope sediment transport process in steep arid and semiarid landscapes' (Gabet 2003). Movement of rocks with meltwater, common in spring or after summer snowfall, can also occur after rainstorms under 'no-snow' conditions. These operators are commutative in that they can be added and multiplied, although a problem for geomorphic investigations is determining the quantities, rates and fluxes, of material moved. Heights above sea level are derived from Google Earth and marked as $\sim$ m and map lengths, from GE Ruler tool, in m or km.

Table 1. Mapping digraphs, denoting mountain geomorphological features in a landscape $\mathbb{LD}$, includes mountain domain, $\mathbb{Dm}$, in this paper. Locations can be placed on a map, satellite/aerial image or terrestrial image and location identified with a [dLL]. Italic typefaces are used in a sequence of material transfers and when used with geomorphic operators as in the text. The order in this table is roughly highest to lowest altitude.

Digraph	Feature, brief description, cognates and use. Any digraph can be used on a map/image and geo-located by [dLL] as appropriate*. The list is roughly altitude located from mountain top to valley
$\mathbb{LD}$	Landscape domain, landsystem area investigated. General designation for an area, may include selected landforms as appropriate. $\mathbb{LD}$ also acts as an information container, {$\mathbb{LD}$}, for many attributes; location altitude range, vegetation, meteorology, climate etc as required as also data/author sources. Subset is mountain domain, $\mathbb{Dm}$.
AR	Arete (= ridge crest) may be start of a transect (e.g. above **FF)** identified by [dLL]
FF	Free face, rock slopes + free rocks and including snow patches (**FF** covered in winter)
CO	Couloir (= ravine, steep gully) generally cut in a rock free-face
SS	Scree Slope, (talus) of weathered debris at a resting angle, usually 30–35°
GL	Glacier perhaps with snow/firn or bare ice identified by high albedo
GLd	Glacier, with some visible debris (weathered rock) on the surface.
BR	Bare rock might be identifiable at some localities, generally at lower angle than the **FF**
RG	Rock glacier, distinctive flow forms and steep snout, location identified by a [dLL]
RG.p	Rock glacier, with meltwater pools (**.p**) on surface, ice cliffs (**.i**) showing through debris
RGf	Rock glacier, fossil, presumed no current active flow, low-angle snout, may be vegetated
RGs	Rock glacier, snout/front identified by a [dLL] tuple (specify stable/unstable if necessary)
ML	Moraine – distinct ridge, Lateral location; **GL** may no longer be present
MT	Moraine – ridge in 'terminal' location, sequences identified by **MT1** (oldest), **MT2** etc, usually in order of deposition. Size of feature specified additionally. Absence of feature denoted by (~~MT~~) (strike through, not bold) if necessary
DA	Discrete Debris Accumulation, undifferentiated debris of indistinct morphology
PL	Protalus Lobe (also small, valley side rock glacier), may or may not have 'flow' features
PR	Protalus Rampart, distinct ridge (may or may not have a snowbanks or patches above)
SP	Snow Patch, generally 'permanent' or persistent over seasons
RF	Rockfall scar, track, deposit; on glacier **RF**(**GL**), use → operator if required.
FA	Fan on or as part of **SS**, usually below a gully or couloir in bedrock
OW	Outwash, undifferentiated **GL** foreland with fluvial sediments, little/no vegetation
VF	Valley floor, low-angle slope/area, can merge with other forms e.g. **OW**, **TS**
LA	Lake, Water Body, **LAi**:?glacier-dammed; transient feature, (LA) former feature
WE	Weathering, site of particular significance, 'active' weathering, with [dLL]; sample location
*	Location of a feature denoted by [dLL], e.g. **RG.p**[35.91232,71.16742] = pond on surface of rock glacier at location shown. Other suffixes possible if declared

Letter digraphs (Table 1) identify mappable geomorphological surface features used in this paper and can also help summarize material transport sequences (Whalley 2021a, 2021b) and in the text.

Digraphs can be combined as a mapped sequence on a (usually downslope) transect showing landforms mapped on GE or other images; reading downslope, left to right, three sequences of landform elements could be: ***FF:SS:VF, FF:GL:RG*** and ***RF:VF.***

The direction of the transect, in degrees, from a [dLL], [35.9263,71.1180] is given in csv form [35.9263,71.1180],090. Transects are usually along valley axes (thalweg) or transverse to this axis. Reverse slopes, counter to the fall line slope angle, may be used; **SS><SS**, represents a scree or debris slope followed by a section directed upslope. Combined with geomorphic operators, material movement down a transect can be identified, for example in a transport sequence, thus:

- ***FF→SS*** Rock moved from a free-face to a scree slope
- ***FF⇢GL*** Snow/ice moved to glacier
- ***FF→GL↠MT|*** Rock from free face moves to a glacier, ice moves debris to a terminal moraine (**MT**) where transport ceases (|, may be left understood).
- ***FF↠GL→RG*** Snow/ice + debris from free face to glacier, debris moved to rock glacier

These sequences are indicative rather than definitive, there is no indication of times, volumes or frequencies of material transfers, although these might be added subsequently as information tensors (Whalley 2021a). This scheme is an extension of facies approach to mapping surficial deposits of Madole (1972) and Richmond (1962). These sequences are discussed with respect to a mountain topographic domain, $\mathbb{Dm}$, after presenting the field evidence.

The idea of 'geomorphic information tensors' (Whalley 2021a, 2021b, 2021c), in which the above sequences may be placed, is a move towards quantifying data on a transect/profile and allowing information on the line to represent change. This might be indicated by placing + or – after an operator to signify increasing or diminishing material transfer along the connectivity line. It means that subsequent studies using, for example DEMs, to allow contributing debris area inputs to be calculated from interferometric synthetic aperture radar (InSAR), Structure from motion (SfM) and UAV (drone) flights to examine features. Remote sensing and machine learning still require appropriate ground truth to facilitate remotely imaged landscapes.

It is convenient to identify transport paths from high to lower altitudes, potential energy, identified as a transect or profile. Landforms can be identified on each line, here identified with symbolic digraph. This allows a 'storyline' to be built in the recognition of 'uncertainty' where a storyline is, 'a physically self-consistent unfolding of past events, or of plausible future events or pathways' (Shepherd et al. 2018, p. 555). With the digraph coding, addition of feature descriptors of landforms or a transect itself, helps to assemble information within a landscape set, $\{\mathbb{LD}\}$. Geomorphic 'information fields' of the area, the addition of information via geomorphic operators, indicates broadly-defined material transfer 'processes'. The use of process 'operators' is a means of adding more information to a $\mathbb{LD}$ in the light of sensitivity and change (Brunsden and Thornes 1979).

Traditional geomorphological observations may suggest unique and unequivocal recognition and designation of **GL** and **RG**. This distinction has been used in machine learning and pattern recognitions procedures to identify permafrost areas by rock glacier identification (Baral and Haq 2020; Hu et al. 2023). However, machine learning has been used to identify both clean ice and debris-covered glaciers from satellite imagery (Baraka et al. 2020), yet geometric form variations may provide problems with operator recognition and recording variance. The **GLd** designation might differ according to the locality. Monnier and Kinnard (2017, p. 494) indicate that, 'debris-covered glaciers are characterized by a chaotic distribution of features evocating surface instability such as hummocks, collapses, crevasses, meandering furrows, and thermokarst depressions and pounds [sic, = ponds?]'. With [dLL] mapping, it is possible to show what, where and when an observation at a location represents. For example, in the present study, ***GL:GLd:RG*** represents a transition from clean ice (accumulation zone) to debris-covered glacier to a rock glacier feature. With these conventions and uncertainties mentioned, summaries of landsystem information in the study area can be developed.

The advantage of this methodology, especially using [dLL], is that anyone in the future can examine the evidence and re-examine the data, especially if there is new imagery or new techniques become available, For example, SfM could be used to examine material movement on a transect. If these data are recorded, then the data become more accessible and re-usable using the FAIR principles (Whalley 2023a).

Field area location

Figure 1 shows the continental Karakorum-Himalayan mountain ranges with peaks up to 8000 m high in the Karakorum but 5–7000 m above sea level (asl) in the western and more continental climate of the Hindu Kush (HK).

Field investigations on rock glaciers in Central Asia are sparse but include studies by Grötzbach (1965) and Mayewski et al. (1981) from Kashmir [L5]. Under similar climatic conditions, studies of rock glaciers in Iran and Turkey are given by Schweizer (1970). Blöthe et al. (2019) provide an inventory of rock glaciers in the HK and other ranges, although individual features are not identified to make landsystem comparisons. The review of current glacier status by Joya et al. (2021) includes a mention of debris-covered glaciers but not rock glaciers. Gilbert et al. (1969) report field exploration of a small HK glacier, Mir Samir [L6] 50 km to the west of the present study. The GLIMS, Global land Ice Measurements from Space (Raup et al. 2007), and Randolph Glacier Inventory (RGI) identification are included in the following discussion where appropriate.

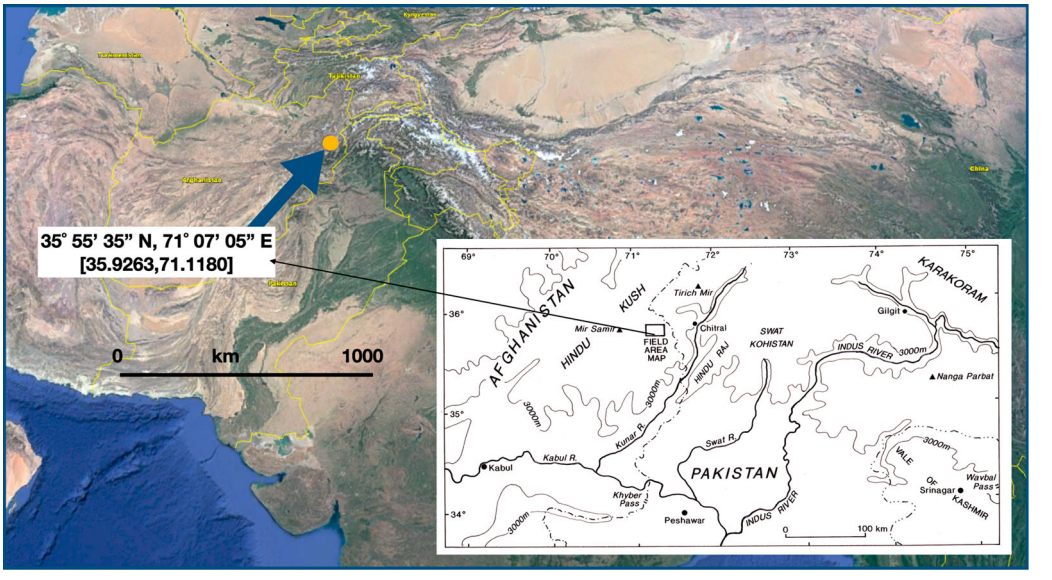

Figure 1. The mountains of Central Asia. The study area in eastern Afghanistan (Nuristan) in the Hindu-Kush range is arrowed on a Google Earth image with co-ordinates in traditional Latitude/Longitude and in decimal format [35.9263,71.1180]. The title of the paper gives a two-decimal version; [35.92,71.13]. Main image ©Google Earth.

Both glaciers and rock glaciers were known to occur in the Bashgal area of Nuristan (Tranter 1968) but return since 1976 has not been possible for security reasons. The areal density of rock glaciers in this region appears to be as high as for any mountain area reported in the literature. The range of glaciers and rock glaciers in the Upper Bashgal provides inter-relationships to test the permafrost mapping of Schmid et al. (2015) and the utility of the comparative landsystem mapping approach.

Study area: detail setting

The study area (Figure 2) includes the Suigal, Shoshgal and Peshashgal basins of the Bashgal River (Kashiragal Darah), a tributary of the Kunar in eastern Afghanistan (Figure 1). The $\mathbb{Dm}$ has complex geology; schists, gneiss, granites and granodiorites up to 6500 m asl. The climate is continental with little summer precipitation, only occasional monsoon incursions (Sivall 1977) and high summer air temperatures (Bowlby and White 2019). Snowlines were found by Grötzbach (1965) to be 4700 and 5100 m asl on north and south facing slopes respectively in the Khwaja-Muhammad region, 100 km west. The generalized map of Grötzbach and Rathjens (1969) implies a snowline of 5200 m asl for the Bashgal area, suggesting that the permafrost zone is likely to be above about 5000 m asl. The transient snowline on the upper glaciers reached approximately 5600 m in mid-August 1976. Snowfields on the high peaks feed glaciers directly and by avalanches from steep rock faces. No glacier mass balance observations have been made in this area but Gilbert et al. (1969) give basic background data from the topographically similar Mir Samir area. Winter snow accumulation is known to be high but starts to melt rapidly in May and June. Gilbert et al. (1969) found that the larger, north facing glaciers, had a lower limit at about 4800 m asl. Although, the glaciers in the Mir Samir region are rather smaller (typically <1.5 km^2) than those in the Upper Bashgal, their response to the general glacier retreat found in the Hindu Kush area appears similar. Maharjan et al. (2021) provide a summary of mainly remotely sensed data confirming the general recession of glaciers in Kunar province and Afghanistan since about 1960. Although glacier recession and melting/down-wasting have been monitored by satellite imagery, little is known about precipitation changes over the last 100 years; generally, positive winter mass balances lead to glacier advances.

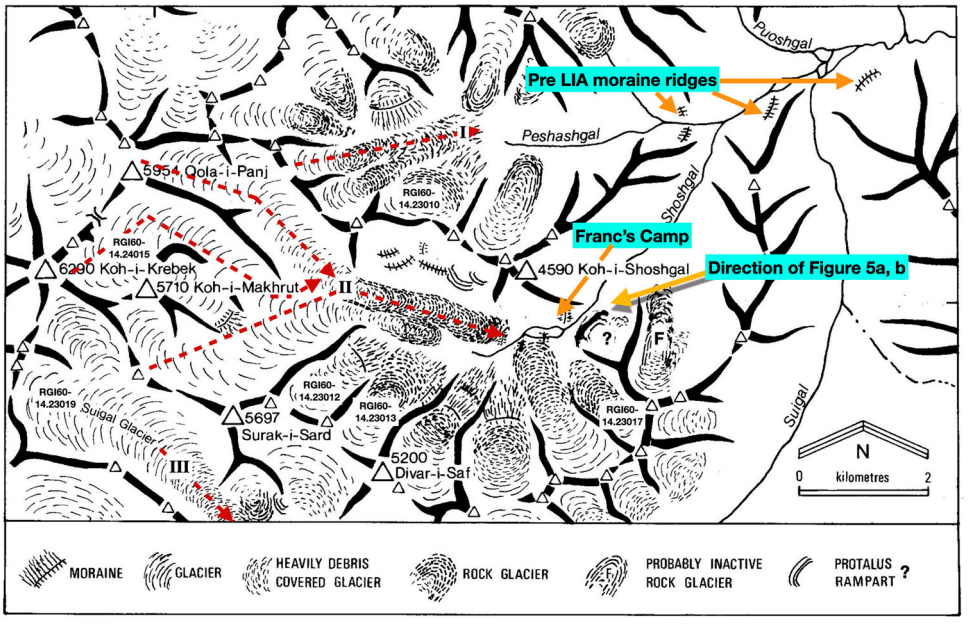

Figure 2. General Map of the study area centred on Koh-i-Shoshgal [35.9369,71.1313] derived from topographic map and field observations. Main valley glacier profiles (I, II, III) are shown. Also shown are selected glaciers from the Randolph Glacier Inventory (RGI–) determined from the World Glacier Monitoring Service interactive map.

The following sections use transects to examine topography the complex sediment transport systems. The dating of moraines and ice-free surfaces in the Mir Samir region (Gilbert et al. 1969) suggests an age of less than 400 years for the Little Ice Age (LIA) in this region, associated with relative dating of rock surfaces with debris varnish cover coloration.

Main valley landsystems

Figure 3 shows three valley systems, long profiles I, II and III, annotated on Google Earth to show significant features and their [dLL] locations. Main valley axis sections are termed profiles with transects referring to side valley tributaries. Origins of profiles and transects are located by a dLL tuple and a bearing from that point.

The high snowfields feed accumulation areas of glaciers in the main valleys on which rock debris is transported supraglacially. Field evidence for pre-Little Ice Age (LIA) glaciers is poor (Porter 2011), although high elevation moraines were identified on valley sides (Figure 2, m) they were not investigated. The ice of Late Pleistocene valley glaciers would have filled the cirques in the high mountains, today substantial areas of ice-free slopes of weathering bedrock exist above the glaciers (e.g. Figure 3). Three long profiles are used (Figure 2) with starting points identified in [dLL] format in Table 2.

Profiles II and III have separate arms to account for bends in the valley and (Figure 3) the converging glacier area has additional arms and contributing areas. (These have been mapped as part of the GLIMS project and it appears that glacier, rock glacier and debris-covered glaciers are *all* included in the mapping.)

The main valley glaciers profiles (I, II and III) have no distinct lateral or terminal moraines with sharp crests and 'ablation valleys' nor do the glacier snouts lie between substantial lateral moraine systems, as for example, Khoistan [L7] about 180 km east. The exception is in profile II where there are distinct lateral moraines, although these occur 1.5 km above the present snout (Figure 4).

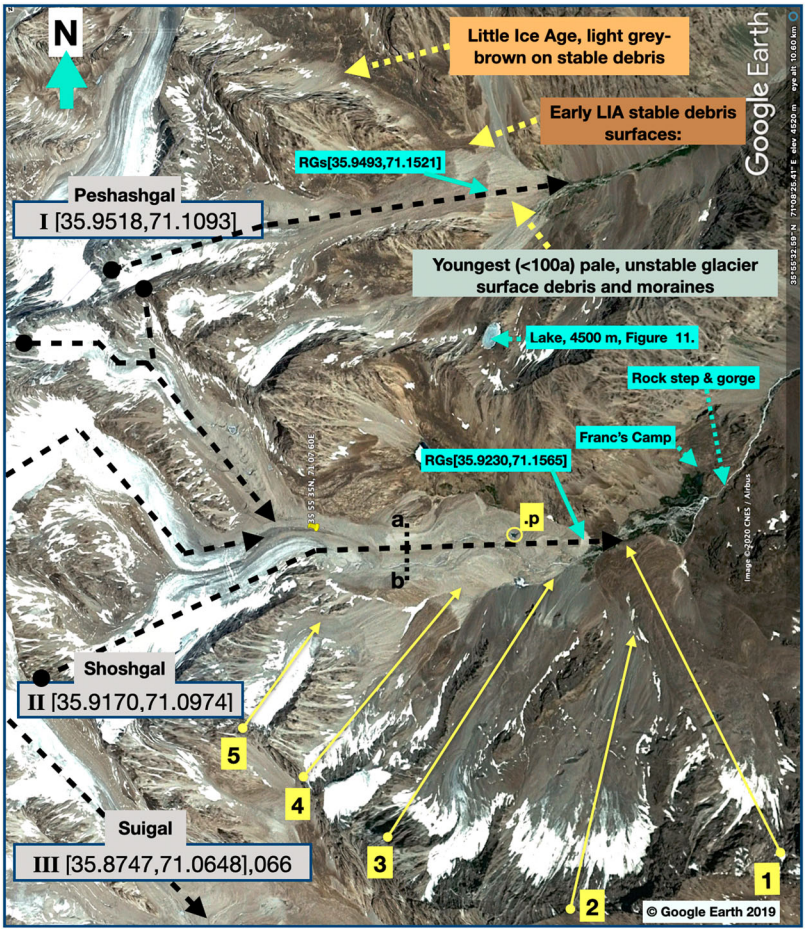

Figure 3. Overview of the main part of the study area, with profiles I and II, starting points shown (Suigal, profile III bottom left). The approximate relative ages of surfaces are provided by rock varnish coloration: LIA debris on glaciers is light grey and distinguished from the darker weathering of stable cliff surfaces. Circled on profile II is a surface meltwater pond (**.p**) missing from current 2019 GE images. Cross profile a–b is shown in Figure 4. The colour saturation may vary between images. The location of the 'pin point' is [35.9267,71.1309]. Solid arrowed lines, 1.–5., are transects shown in Figure 5. Image: ©CNES/Airbus/Google Earth 2022.

The terminal positions are marked by steep rock glacier/moraine, snouts. An example is at the end of profile II at [35.9230,71.1565] ~4175 m asl. This suggests that glacier ice was gradually covered by surface debris from cirque headwall free-faces (**FF**), generally merging with the main trunk glaciers becoming **GLd** features and gradually becoming distinct **RG** with steep snouts: **RGs**

Table 2. Basic information on the three valley system profiles. The third element after the tuple is direction/bearing from origin. Height and location data from 2019 Google Earth CNES/Airbus images.

Valley label: name	Traverse origin & direction tuple	Feature mapping profile	Randolph Glacier Inventory	Approx. height of snout/terminus m asl (2019)	Comment (Area, RGI)
I Peshashgal	[35.95183,71.10938],095	***GL:GLd:RG***	RGI60-14.23009	**RGs**[35.9493,71.1521] ~4190 m & Fig. 3	RGI includes 'fragments'
II Shoshgal upper	[35.91702,71.09742],074	**GL**	RGI60-14.24015		~3 km long (4.46 km^2)
II Shoshgal, lower	[35.92500,71.13134],096	***GL:GLd:RG***		**RGs**[35.9230,71.1565] ~4190 m	~2.6 km long
III Suigal upper	[35.87472,71.06481],066	**GL**	RGI60-14.23024		~4.8 km (4.3 km^2)
III Suigal lower	[35.89200,71.11397],107	**GLd:RG**		**RGs**[35.8845,71.1443] ~4170 m	~3.5 km long

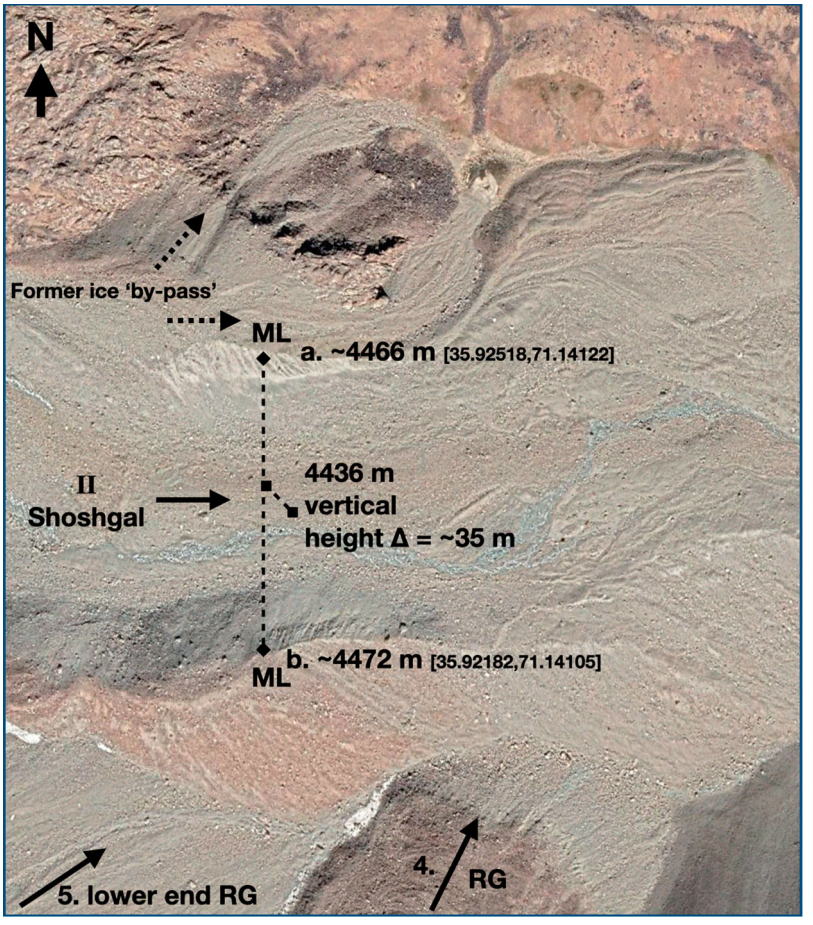

Figure 4. Lateral moraines (**ML**) at locations a. [35.92518,71.14122] and b. [35.92182,71.14105] ~360 m apart and some 35 m above the debris-covered surface of the Shoshgal glacier (Profile II). This height difference is due to the flow reduction since the moraine emplacement (early LIA?) but has allowed the glacier to become more channelized, increasing the snout extension. ©Google Earth.

[35.9493,71.1521] at ~4190 m asl for Peshashgal (Profile I) and **RGs**[35.9230,71.1565] ~4190 m asl for Shoshgal (Profile II).

Rock glacier tributaries of the Shoshgal (II)

Figure 5 shows six transects, five into the Shoshgal valley (Figures 2 and 3) and summarizes a GE interpretation showing cirques and glaciers with surface-emergent debris, originally deposited by (slush) avalanches (fluvial talus, Rowley et al. 2015, p. 421) and debris falls from the **FF** to **GL** surfaces. The processes apply to the geomorphic operators:

- ⇢ snow deposited, probably from winter storms, moved to lower elevations by snowfall, snow avalanching and wet avalanches in spring. Such avalanching will also transport solid rock debris and this flux may well have been higher in the early LIA.
- → solid debris moved by slush avalanches and free fall of debris weathered from the free faces, even in summer [35.9149,71.1252].

For the most part, these operators work together according to the season, meteorological conditions and weathered rock availability. The cirques operate individually and currently add no ice or debris

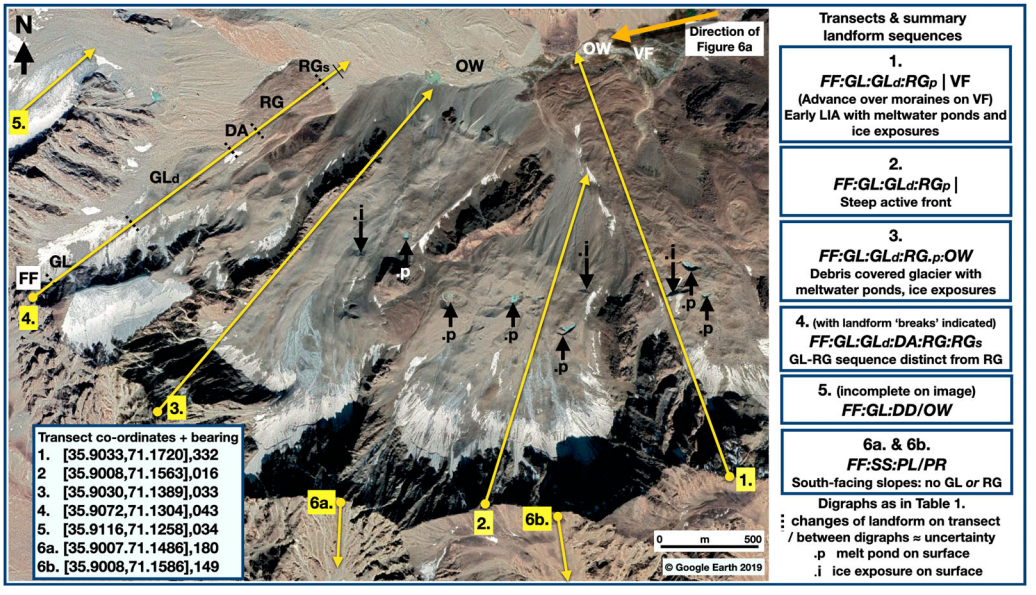

Figure 5. Transects 1.–5., north to the Shoshgal. Transects 1. and 4. terminate in distinct, dark coloration, rock glacier snouts. Transect 4. terminates in an active front slope, possibly still advancing (Figures 2 and 3). Transect 3. Is advancing over outwash (**OW**) Only transect 4. is demarcated into components. Meltwater pools and surrounding depressions (up-arrow, **.p**) can be seen on Transects 1., 2., 3. with ice cliffs showing through debris cover (down-arrow, **.i**). Transects 6 a., b. (towards the Suigal, III) have scree slopes (**SS**) on the other (south-facing) side of the ridge with no **GL** or **RG** components. Image ©Google Earth.

to the main glacier system (II). Snowmelt and rain runoff to rivers is contributed but not estimated here.

Figure 5 shows five transects on north-flowing cirques in the Shoshgal valley together with detailed landform element sequences. Surface melt pools (**.p**) occur and show melting of glacier ice below the debris cover. Notably, transects 1. and 4. terminate as steep **RG** snouts with equivalents as debris-covered glacier snouts (**GLd**) for transects 2. and 3. Transect 5. (see also Figure 6(a, b)) terminates in a long and steep, but apparently stable over 40 years, frontal slope. The steep snout/debris slope of transect 5. can be seen on the right. The stability of the circled boulders either side of the arrow can be seen on the 2019 GE image (inset). The light grey surfaces suggest late LIA to present deposition.

Inspection of profiles and transects suggests two main phases of glacier extension, the first producing terminal moraines (**MT1 and MT2**, Figure 6(b)) and a subsequent event that produced the LIA moraine of transect 5. (Figure 6(c)) at altitude and the advancing rock glacier terminus of profile II. The observations now allow an initial investigation of debris movements and accumulation down main and side valleys.

Interpretation of landform elements in profiles I, II and III

The main valleys are shown in Figure 2 and data in Table 2; north to south: I Peshashgal, II Shoshgal (Figure 3) and III Suigal being of similar configuration they would appear to respond similarly to mass-balance changes. The glaciers in the system, as seen in GE, are best thought of as 'LIA' glacier systems as they have very little surface weathering (Figure 4). Although we do not know how (or precisely when) the LIA glaciers started to advance this may have been a rejuvenation of pre-LIA, glacier systems. Grove and Switsur (1994) give evidence for moraines from glacier advances during the Medieval Warm Period before 1465 AD in the Alps and, tentatively, from the greater Himalaya. Evidence in the study site appears very variable and glacier response to weather patterns

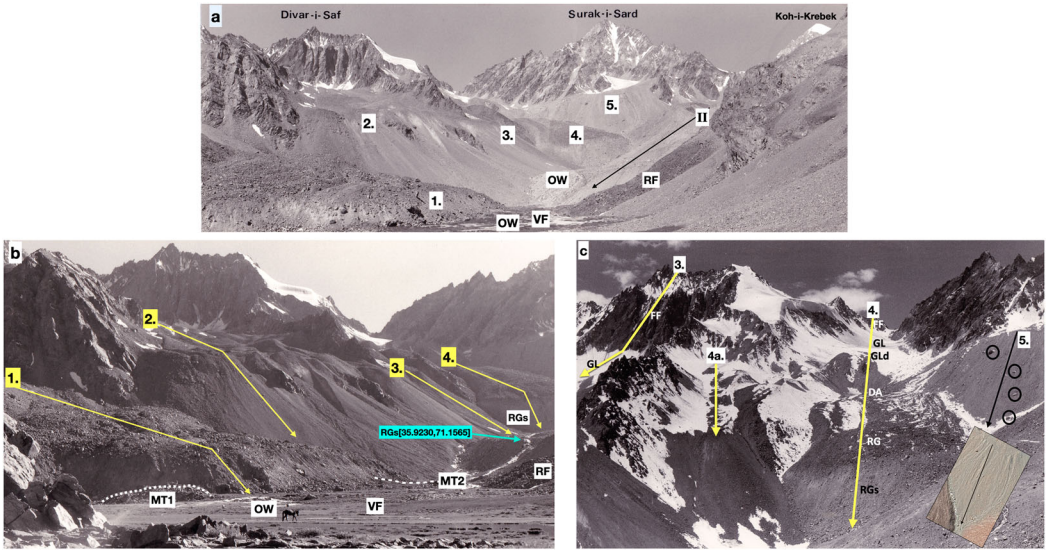

Figure 6. (a) Panorama of features identified in the upper Shoshgal Valley location and view direction [35.9261,71.1677],265 from 'Franc's camp' in Figure 2. Surak-i-Sard is some 7.5 km away, Koh-i-Krebek just appearing on the right. Features identified (and on Figures 2 and 4): Height (from Open Street Map and GE) of the viewpoint is ~4100 m asl. (**b)** From similar location of 5a but with different lighting conditions. Transect 1. (lower portion) descending to the valley floor and over-riding terminal moraine (**MT1,** cross-profile top surface, dotted) and **MT2**, (profile across the valley shown dashed). The lower portions of transects 2., 3. and 4. are also shown. On the left is a rock outcrop at the high valley step covered in dark rock varnish. The lower portion of a (dark coloration) rockslide, **RF**, on the right. (c) Looking up transect 4 showing the transect of Figure 5. Shown as two portions: upper ***FF:GL:Gld*** and, at about the same surface elevation (~4400 m. asl), of the transect, a discrete debris accumulation, ***DA:RG:RGs.*** Transect 4. ***FF:GLp:RG*** [35.9083,71.1401],028,**.p** at 580 m asl from origin (@2019). All images 1976 ©W.Brian Whalley CC BY-SA 4.0 2024.

across the HK-KK ranges varies according to glacier size and continentality. Current climatic conditions in the study area have no monsoonal effects, snow accumulation from winter storms with ablation by sublimation at high altitudes (shown by névé penitentes) surface melt at lower altitudes. It appears from the lack of frontal (**MT**) and lateral moraine (**ML**) systems that these glacier tongues (for I, II and III) are still advancing down valley floor (**VF**) over meadows and outwash (**OW**) (Figure 6).

Although the glacier limits of the 'Late Pleistocene' (pre-LIA) glaciers are not known, traces were identified on high valley sides (Figure 2). They usually show as slight ridge features on the ground and are difficult to identify in GE. There are small loop (**MT**) moraines in the lower Peshashgal valley and also near the rock step at 'Franc's camp' (Figure 6(b)) ~4100 m asl in the Shoshgal valley [35.9257,71.1672]. These are distinct ridges suggesting that the glaciers were largely debris free. The moraines **MT1** and **MT2** (Figure 6(b)) near the rock step are probably cross-valley remnants of a pre/early LIA glacier with relatively low surface loads compared to the active **GLd** and **RG** glacier snouts that currently terminate these glaciers. This contrasts with the high debris fluxes of early LIA advances in the European Alps (Whalley et al. 1996).

With increasingly reduced snow accumulation, high mountain rock slopes above the glacier surfaces would extend their free face areas – such as in high mountain ranges throughout the world outside Antarctica. Debris accumulation from the highest rock faces was passed down the main glaciers, becoming **GLd**, and gradually thickening to become **RG** (Figure 3). The debris thickness insulates the glacier according to its thickness (Whalley 2020). Unlike many present-day debris-covered glaciers in the Alps or New Zealand, there are no distinct lateral moraines with a debris-laden glacier snout between them (L8). The Bashgal glaciers and snouts look similar to the glacier-rock glacier 'transitional' landforms in the Andes such as described by Monnier and Kinnard (2017) [L9], with similar continental, high-altitude glacierized systems.

Himalayan glaciers have been losing glacier mass since the LIA (Mayewski and Jeschke 1979) although Bolch et al. (2019) note that some glaciers in the Hindu-Kush Karakorum may be static or gaining mass. The ***GLd:RG*** components of profiles I, II and III show glacier surfaces becoming increasingly covered with debris, thereby reducing ablation and affecting their mass balances. However, Figure 3 shows a surface melt pond down to the glacier surface of II and this effect is expected to become increasingly common as it is with several of the 'Dry Andes' rock glaciers (Whalley 2023b) and Monnier and Kinnard (2017). Such melt ponds (**.p**) are well-developed on some of the tributary ***GL: GLd:RG*** profiles (Figure 5).

The right-hand side (north-flowing) contributing cirques (Figure 5, transects 1.–4.) are all debris-covered glaciers, leading to rock glaciers in their lower portions. The exposures of glacier ice below (**.i**) and meltwater ponds (**.p**) show the continuity of glacier ice into the rock glacier portions. The steep front of 1., **RGs**[35.9221,71.1610], has continued over the 1967–2019 period. The identifiable boulders at and below the steep snout have not been observed in GE whereas they have for the snout of 5. This suggests that 1. is still advancing as **MT1** cannot now be seen. A terminal forward movement of 0.5 m/a over 40 years would give an advance over the valley floor of 20 m, enough to cover **MT1**.

None of the ***GL:GLd:RG*** systems 1.–4. (or ***GL:MT*** in 5.) appear to have contributed to the main longitudinal transect glacier (II) as they are now distinct from it. During early or pre-LIA glacier times however, they *may* have been joined, but with little surface debris. Glacier system 1., being furthest down the main valley axis, has dark brown surface debris. For 2., 3. and 4. the balance of debris transported by glacier ice has resulted in the ***GLd:RG*** sequences seen. Notably, transect 5. has a 'conventional' ***GL:GLd:MT*** sequence but with a substantial snout debris accumulation with the appearance (and coloration) of a LIA **MT**. Upstream (westwards), from glacier 5. the high peaks contribute to the main Shoshgal (II) valley glacier.

Taken as a landsystem, the Shoshgal (Figures 3, 5, and 6) shows the main valley system responding to pre-LIA glacier down-wasting and recession with increased rockwall (**FF**) area exposure as glacierized area declined. Correspondingly, the output of weathered debris increased as cirque backwall areas became relatively ice-free, i.e **FF**→+. The debris supply might be transferred to either **SS** or **GL** components with an increase in insulating debris on glacier surfaces. On the main valley systems, this insulation appears to be very effective and preserves advancing rock glacier fronts (Figure 6). Only the highest glacier basins fed ice to the trunks and produced steep debris snouts. This configuration also appears in the Peshashal (I) and Suigal (III) systems. The highest basin (5.) is essentially a small glacier with a moraine (~4600 m asl). The rock glacier in transect 10., described below, has its **MT** and **RGs** termination at ~3820 m asl.

The continuity of rockfall debris (**FF**) to surface debris of glaciers (**GLd**) is evident throughout these glacier-debris systems. The suggestion is that the *first* advance of LIA glaciers had very little if any surface debris as the high mountain walls were ice-covered (i.e. **GL** entirely). If we estimate the average surface velocity as 50 ma^{-1} then an ice element moving the 6 km from top to bottom would take only about 120 years and produce a single moraine (**MT**) at the terminus. After the first advance, and perhaps with declining snow accumulation at altitude, more rock exposed after glacier melt became a debris-supplying free face (**FF**→+). The **FF** area available to supply debris to the glacier surface becomes supraglacial down valley and explains the debris continuum. The increasing thickness of the lower glacier's debris cover would allow snout advances to occur.

Side valleys with small glaciers behaved as independent sources of glacier ice and debris accumulation. The lowest altitude (1.) system has maintained a thick debris cover to the (advancing) snout but with some **.p** and ice exposures (**.i**) in the upper section. The ***GLd:RGp*** area has surface melt pools. This also appears to be the case with other high-altitude zones as remarked below (Figures 7 and 8).

Moraines and rock glaciers as part of debris supply connectivity

The sequence of landform elements on the main valley thalwegs (I, II, III): ***GL:GLd:RG:RGs|*** is equivalent to ***GL:GLd:MT|***. That is, surface debris accumulates increasingly towards the snout

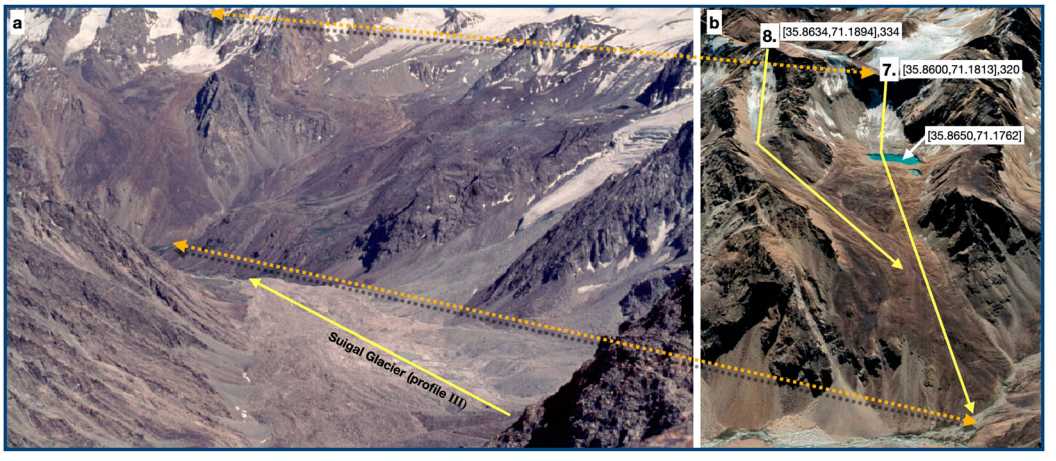

Figure 7. (a) View down the main Suigal valley (III), view from approximately [35.936,71.081] towards the southeast, 1976 image. (b) 2019, steep **RG** descending to the valley floor with no apparent surface meltponds. The headwall glacier has markedly reduced in size over 40 years and the free-face area increased. The large melt pond [35.8650,71.1762], some 0.4 km^2, at the foot of the crevassed glacier will probably increase in size, link with other ponds and escape, perhaps catastrophically, down valley. The lake is at what the permafrost model would term the 'rooting zone' of a rock glacier. The inflection on transect 8. [35.8702,71.1854] separates a ***FF:GL:GLd*** system from a **RG** system below. Images a. ©W.Brian Whalley CC BY-SA 4.0. and b. ©Google Earth.

and a terminal moraine is the equivalent of a rock glacier snout. The terminological distinction between ***GLd:RG*** is arbitrary. No permafrost creep at a 'rooting zone' is required. This behaviour is consistent with a sequence; ***GL:GLd:RG***, depending upon the relative fluxes of ice and debris responding to melt conditions and debris protection to the glacier surface. Unlike the large glacier systems of the Karakorum and further east, the effects of glacier mass balances and debris production of datable moraine systems are unknown. A debris-covered snout allows the glacier to flow further down-valley than if uncovered. This explains why rock glaciers generally reach lower altitudes than glaciers with thin ice snouts or simple terminal moraines, see for example Figures 7 and 8. Transitions between ***GLd:RG***, e.g. Monnier and Kinnard (2017) and Lilleøren et al. (2022, are only dependent on ice and debris supply balances. As 'temperate' (near pressure melting point) ice can be sustained in this way, glacier sliding as a component of velocity is expected. The examined trunk valleys are unusual in that the glacier system does not have distinct lateral moraines near the snout as is typical in the Alps where the large moraine ramparts are thought to have been produced by the deposition of supraglacial debris in the early advance of the LIA glaciers of similar size (Whalley et al. 1996) [L10]. This can be explained according to the relative ice movement and debris supply. Profile II only has distinct lateral moraines well above the snout where glacier flow has been restricted (Figure 4).

This landsystem analysis shows that rock glaciers *are* glacier ice-cored terminal moraines. Lateral/terminal moraine are deposited where the surface debris exceeds the potential of a glacier to remove this load. This simple explanation allows a variety of landform configurations in $\mathbb{D}\mathbb{m}$, to be formed and exist without permafrost.

Neighbouring valleys: further evidence for the glacier ice supply model

Further information on the Suigal (III) system is shown in Figure 7. The main, axial valley contains a debris-covered glacier in the lower 3 km. Upstream, there are three main, mostly debris-free, feeder valley glaciers. There is one rock glacier system feeding into the main valley in the lower region of profile III having the appearance of a debris-covered glacier (Figure 7), but no surface ponds are visible in the GE image. In the ***GL:RG*** zone there are melt pools developing

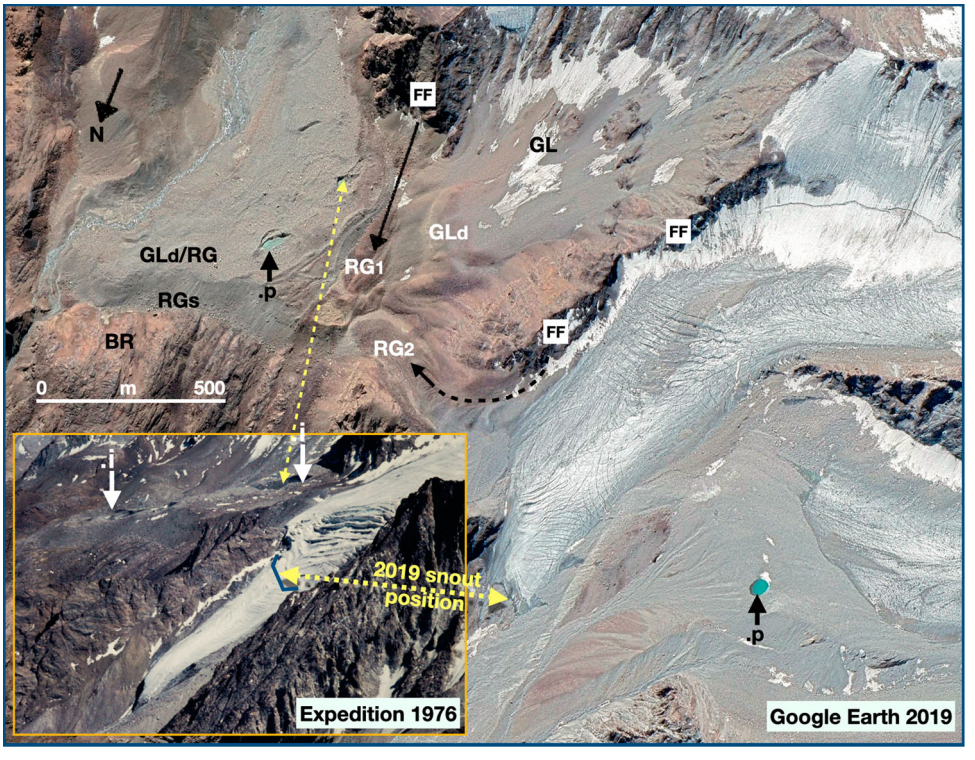

Figure 8. A debris-free glacier tongue flowing to the Suigal glacier (III) in 1976 (inset and Figure 7 left) is depleted in 2019 with its terminus shown [35.8769,71.1328]. Left shows a steep snout, mapped as a **GLd** and **RG**, advancing over bedrock with substantial glacier melting below the debris. The formation of **GL**, **GLd** or **RG** depends entirely upon the volume of debris that can cover the glacier ice. Main ©Google Earth, Inset ©W.Brian Whalley CC BY-SA 4.0 2024.

into large ponds at ~4550 m asl, [35.8650,71.1762]. The lower reaches of **GLd**[35.888,71.124], which terminates ~4160 m asl, is a complex set of lobes with tributaries to the area of **GL**, **GLd**, **RG** and **SS** with **OW** on the valley floor.

In the upper reaches, Figure 8 shows the melting of a clean, steep glacier tongue in 1976 has retreated at the same time as the production of melt ponds (**.p**) in debris-covered glaciers. Such glacier melting can be seen in the vicinity of [35.8601,71.1819] with some glaciers [35.8518,71.1838] being substantially debris free, the neighbouring **RG**[35.8548,71.1942] has a thick debris cover, no**.p** or**.i** and no exposed bare ice: ***FF:SS:RG***.

Figure 8 also shows how rock glaciers can form by switching on (+) debris supplies in relation to glaciers. At **RG1**[35.8690,71.1375], a rock glacier has developed from debris from the **FF** over ice in the depleting volume in the cirque, centred on [35.865,71.131]. The rock colour shows that **RG1** developed earlier than the neighbouring **GLd**. Debris from the **FF** on the right-hand side of the major debris-free tributary of Figure 8 formed a diffluent feature, **RG2**[35.8713,71.1365], as the ice supply was cut off during down-wasting.

Lower valley debris transport landsystems

Below the Shoshgal rock step and gorge, [35.925,71.167] at about 4100 m, several debris transport systems are seen on the south of the valley axis. These are represented in Figure 9 and summarized in Table 3. The surface varnish indicates relative ages of the features and bedrock and rockfalls (RF).

How far debris extends towards the valley floor on transects 10a,b,c. depends on the balance of debris supply to glacier surfaces available. For transect 10d the ice accumulation area was very small

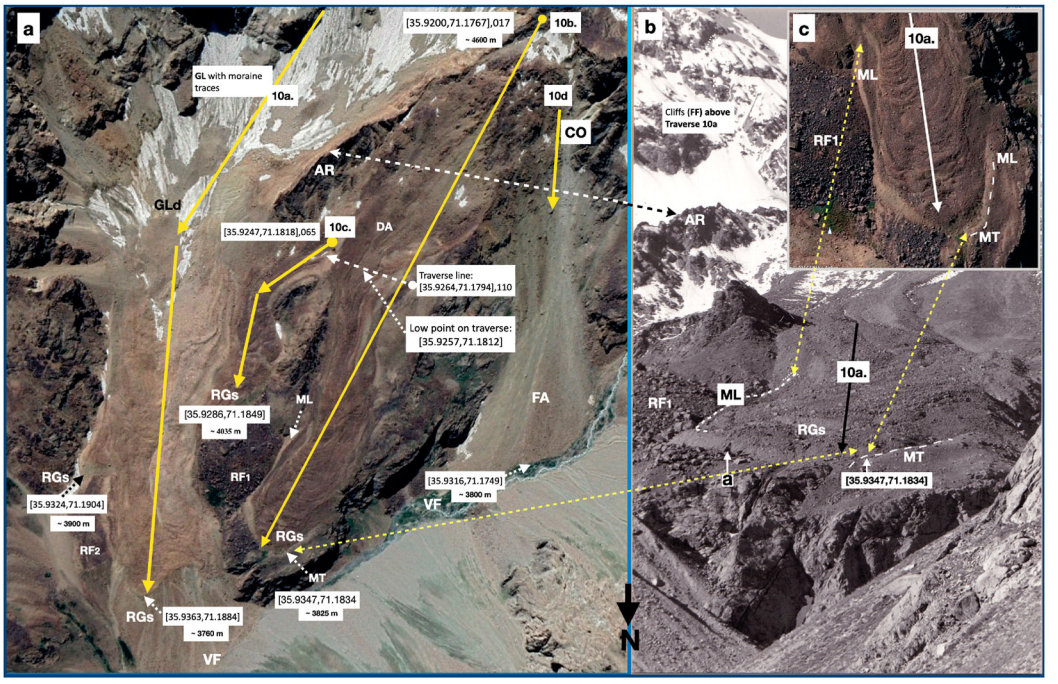

Figure 9. Comparison of Google Earth (a, c) and 1976 (9b) views of a debris transport systems on the south bank of the Shoshgal. Dashed double arrowed lines connect features on each image. Transect comparisons are given in Table 3. (a) Dark-coloured debris surface can be used to delimit debris movement paths for transects 10a, b, c and d. **RF2** may be a continuation of **RF1**, subsequently over-ridden by the **RG** of 10a. (b) The lower part (500 m) is shown in the GE insert of the 1976 image with detail in Figure 10(d). (c) Outside the **RG** of 10b, a terminal moraine **MT** [35.9347,71.1834] ~3825 m asl, also marked in the GE image together with a right lateral (**ML**) moraine within which (top of Figure 9(c)) the **RG** has over-ridden and then flowed down to the moraine limit. This suggests an early/pre – LIA advance with little surface debris to form the moraine and a subsequent LIA glacier advance with substantial surface debris load to produce the **RG**. Images a. and c. ©Google Earth, b. ©W.Brian Whalley CC BY-SA 4.0 2024.

so weathered debris supplied through the couloir (**CO**) just forma a fan (**FA**). This fan shows no flow features that might require designation as a **RG**.

The **RG** flow divergence, separating 10 b from 10c, has produced two distinct lobes as the ice supply to 10c was depleted. A similar flow divergence can be seen at [35.8707,71.1375], is like others in the literature at various scales [L11] (Whalley 1976).

The transverse line [35.9264,71.1794,110] across transect 300 m across the feature shows two lateral margins (equivalent to **ML**) with a depression between at [35.9257,71.1812] where the glacier surface has lowered between moraine ridges (cf. Figure 4). This non-isovolumetric depletion indicates a previously greater glacier thickness which allowed the spur rock **RG** to flow from [35.9247,71.1818,065] to **RGs**[35.9286,71.1845]. The concave transverse surface can be explored

Table 3. Summary of debris transport landsystems on the south of the Shoshgal (II) (Figure 9).

Traverse	Digraph Description	Features/Comment
10a	***FF →GLGLd:RG***	**GL** receives debris becoming **RG**, active **RGs**, recent feature, reaches to **VF** in main valley due to continuing debris and ice supply,
10b	***FF:RG***	Possible RGs advance to previous **MT** position of earlier **GL** extent. depleted ice and debris supply; no longer exposed glacier ice, much older than 10a
10c	**RG|**	Originated from 10b but ice supply depleted at flow divergence; **RGs** well above that for 10b due to limited ice supply
10d	***FF →CO→/→FA|***	No area for **GL** formation, steep slopes just supply debris though **CO** for continuous **FA** development to present day reaching **VF**. No indications of **RG** flow structures.

using the GE Ruler/Path tools and shows the depletion of glacier ice melting vertically down as well as moving downhill under its insulating debris cover (Whalley and Palmer 1998) (L12).

The **DA** (discrete debris accumulation) on 10b. has developed as the once-existing glacier ice exposure at the head has been buried below the **SS** debris. The **DA** is the 'spoon-shaped depression' of a glacier origin for **RG** (Whalley and Azizi 2003). It is where glacier melting below a thin layer of debris is greater than where the debris provides nearly 100% insulation. This **DA** region is equivalent topographically to the 'rooting zone' of those promoting a permafrost origin (Barsch 1992).

Landforms and processes in the mountain domain

Mountain slopes with no permanent ice/snowcover could be called 'periglacial' or 'paraglacial'. However, these terms are essentially outmoded with little meaning in a time of rapid glacier recession and down-wasting. 'Periglacial' is a legacy from climatic geomorphology and has no explanatory value when considering weathering mechanisms over time (pre – post LIA). In the HK, very high rock surface temperatures promote chemical weathering (Whalley 1984) visible as rock varnish on many surfaces (Figure 10(d)). Weathering 'processes' (time integrated mechanisms) need to be considered via materials/processes/landform/biotic changes (Whalley 2023a). Single terms, like 'periglacial' and 'paraglacial', where sediment fragments have complex time-dependent and process-dependent (degrees of freedom) histories, are insufficient and misleading. Using material transport paths and geomorphic information tensors (Whalley 2021c) provides a better way to identify material movement in the $\mathbb{Dm}$. Thus, in Figures 9 and 10, rock and scree slopes are not related to glaciers but exposed to a variety of weathering mechanisms. Hence, ***BR:FF→SS*** is accomplished by (unspecified) weathering processes ***BR:WE:FF→SS***. The rock varnish coloration (indicative of chemical processes) was reported from the study area (Whalley 1984). In these sequences, the geomorphic operator, ↓ (*in situ* weathering) allows discussion about complex rock weathering mechanisms in $\mathbb{Dm}$ over time.

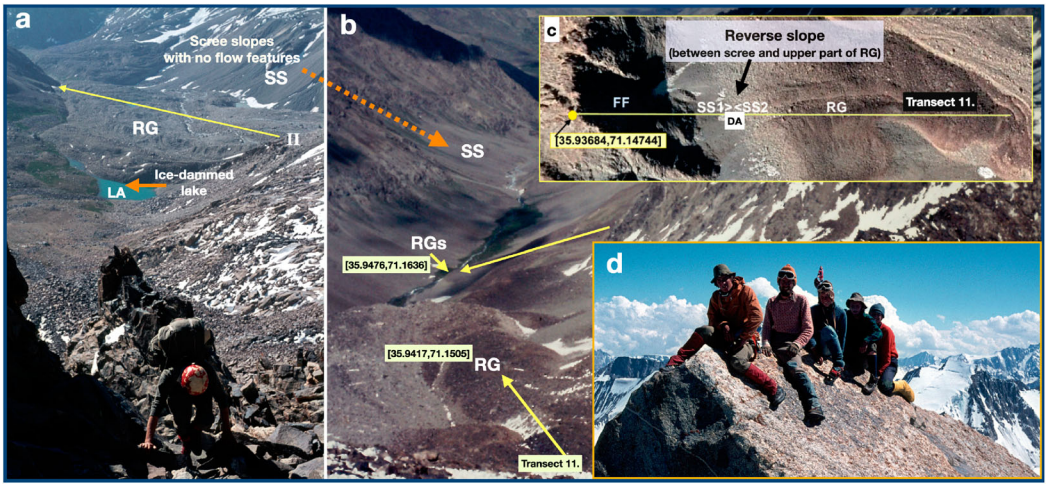

Figure 10. Bare rock and free-face (**FF**) surfaces showing rock weathering and debris incorporation into screes (**SS**) and rock glaciers (**RG**). (a) Looking towards profile II: weathering rock walls connected to scree slopes Weathering ↓, rockfall, dry ravel →, slush avalanches, rainfall/storms. (b) Looking towards the lower Peshashgal valley from [35.9387,71.1406]; scree slopes and **RG.** No 'flow' features are visible on the scree slopes (as might have existed with former permafrost conditions). (c) (inset) GE view of the rock glacier in b. showing the main components on transect 11. In Figure 10(c), transect 11. [35.9368,71.1474],033 ~500 m long shows a reverse-slope, 'spoon-shaped depression', of the down-wasting glacier in scree (**SS1><SS2**) with a low point at ~4435 m [35.9386,71.14895]. See also the discussion relating to Figure 11. Images ©Google Earth. (d) (inset) Rock summit at ~5190 m asl showing rounded rock edges and rock varnish [35.94723,71.11934] indicative of long-term chemical weathering. Images a,b,d ©W.Brian Whalley CC BY-SA 4.0. Image c, ©Google Earth, CNES Airbus, Maxar.

Figure 10 Illustrates ways in which particles (weathered rock fragments) move, rarely a single path and discontinuous in time where operators ↓, ⇢ and → apply. The path may be a response to the prevailing or instantaneous weather conditions affecting the rock-soil strength, and displacement by falling/rolling stones (dry ravel) or by wet/dry avalanhes. Slopes in the summer give little idea of previous conditions and events. Scree build-up is discontinuous but long-term stability is indicated by the surface rock varnish colouration. The transect 11 **RG** in Figure 10(b) has only a small contributing glacier (Figure 10(c)) essentially, ***FF:SS:RG***. This is unlike rock glaciers in the upper valleys where there are clear glacier ice contributions. Figure 10(c) shows that there *was* a **GL** component, becoming **GLd** and reducing in hight as ice below melted giving the reverse-slopes. Further downslope the thick debris cover retains the ice core which has continued to move downslope. The **RG** terminating on the **VF** at [35.9476,71.1636] in Figure 10(b) has contributory glaciers above 4500 m, [35.935,71.157] and [35.936,71.160] about 1.5 km below the extensive rocky cliff faces.

Free face – scree and small rock glacier sequences

Associated with high ridges (**AR**) (~4000–4800 m asl) with no perennial snow/ice, many small **RG** forms are part of the landsystem. Figure 11 shows slopes and **RG**-like features below current glacierized areas around [35.9347,71.1502]; transects 11. and 15. are discussed.

Transect 11. is a ***FF:SS*** sequence followed by a reverse scree slope concavity (**<SS**) some 50-60 m wide leading to a rock glacier: ***FF:SS><SS:RG***. This concavity is the 'rooting zone' of the permafrost **RG** model from where the **RG** itself is derived (Barsch 1996). There is no glacier ice shown in the imagery, although the reverse slope can accumulate winter snow, some of which may be 'permanent' (transect 14.). In the glacier model, this hollow is the 'spoon-shaped depression' that, 'generally lies between the cirque-floor rock glacier, its lateral moraines and the modern glacier surface. The origin of this depression is best explained by differential ablation of an ice tongue protected at its snout by a thick cover of insulating debris, but relatively free of surface debris in its upper reaches' (Outcalt and Benedict 1965, p. 852). The importance of this depression is also discussed by Whalley and Martin (1994) and Whalley and Azizi (2003) where buried ice patches can be revealed (Whalley 2021a) and where the upper part of a small glacier has been buried under a thin scree cover. At such depressions, reverse-slope, localities we expect to see *glacier ice* exposures with continued warming. For comparison there is bare ice exposed nearby on **GLd** [35.9408,71.1443] ~4480 m asl. A similar situation can also be seen on transects 12., 13. and 14. The latter has a larger **RG** at the toe with a reverse slope at ~4570 m asl. Future images on GE should reveal continued ice exposures through supraglacial debris.

The south-westerly transect 15. starts at the ridge (**AR**) across scree to a stable (dark coloration) 'bench' feature, ~4420 m asl, some 60–80 m wide with a low surface slope. This has been designated a protalus lobe (**PL**), although has no flow features.

Figure 12 shows a portion of the left (north) bank of the Shoshgal **RG** (Profile II, Figure 3) and the lower part of transect 15. (Figure 11) with the location of the small, transient ice-dammed lake. Protalus lobes (**PL**) at a. and b. show bench-like features sub-parallel to the valley sides and with no apparent flow structures. The **PL**[35.9275,71.1518] at **c.** is long rather than wide with no flow features and is broadly similar to features higher up the slope (**d.** to **h.**) that have lighter colouration than **a.**, **b.** and **c.** The arrowheads at **j.** show a gap about 20 m wide between the main light-coloured **RG** and the slightly darker slope. The gap suggests that the rock glacier (or as the main valley **GLd**) was the lateral moraine of the glacier and is much younger (i.e. late LIA) than the slopes above. The bench-like **PL** at a. and b. appear as steps down the mountain side. They are similar to the flat-topped valley side rock glaciers of Evans (1993) in the high arctic and the talus terraces of Chandler (1973) (that come down to the **VF** at sea-level). Rather than being 'protalus ramparts' (**PR**) which are generally ridge-like, these features are flat-topped. It is suggested that downslope moving debris, as scree or rockfall, was passively deposited on the surface of a pre-LIA glacier in this side basin. Alternatively, and more likely, the bench was formed by slope-transported debris filling in the

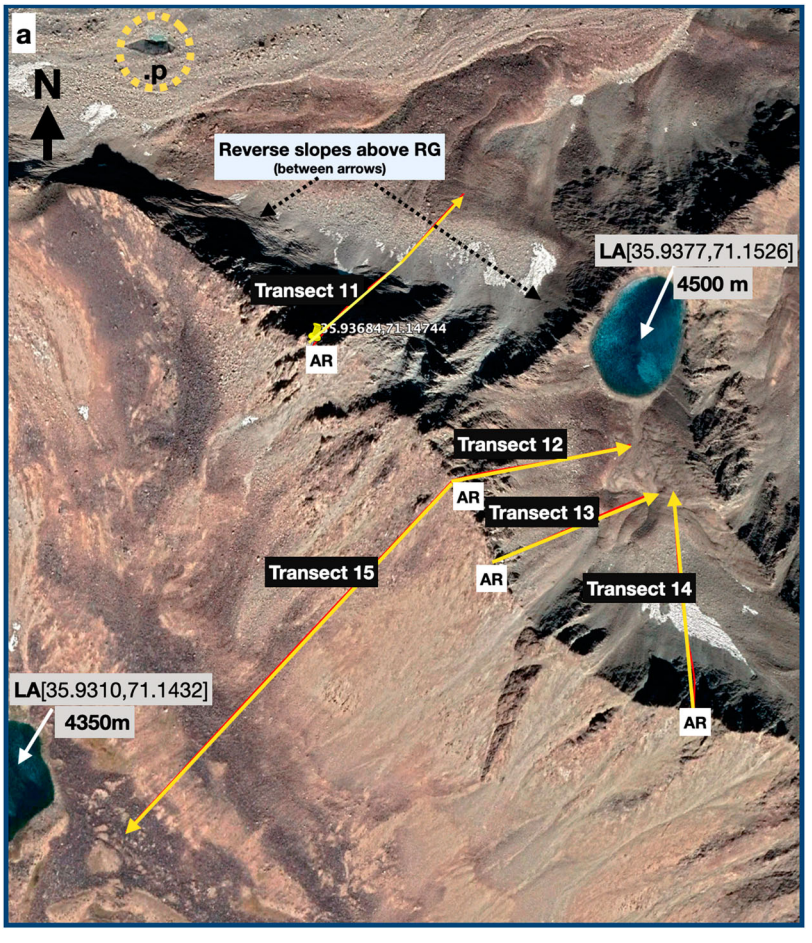

Figure 11. Four north-east facing and one southwest facing transects from ~4500 m asl starting on arete, **AR**, locations. Melt pond at **.p**[35.9409,71.1443] is also seen in Figure 14. 11: [35.93684,71.14744],033 and Figure 10c. A reverse-slope (spoon-shaped) depression is at [35.9385,71.1487]; 12: [35.93544,71.14967],070; 13: [35.93459,71.15045],060; 14: [35.93313,71.15344],355; 15: [35.93545,71.14966],217 and Figure 12. The lake centred around [35.9376,71.1525], 0.2 km^2 and persistent in GE images, does not suggest permafrost exists at this altitude, 4500 m, at the present day. Image ©Google Earth

space between the slope and the side of the glacier. We have noted that the earlier glacier did not have as much surface debris as that during the LIA that formed the present valley and cirque systems. Although the debris protected the ice the overall down-wasting included this debris but with no downslope flow. The rock varnish colouration suggests these features have been stable for a long (probably pre-LIA) time. Figure 12 shows the upper features (d,e,f,g,h) to be much lighter in tone compared with the **PL** on transect 15 and the nearby **a**. and **b.** The lower **PL** terraces appear to be 'kame terraces' between a down-wasting glacier and valley side, as at the classic Muir of Dinnet in Scotland (Gordon 1993) [L13]. These terraces or 'kame moraines' can have kettle holes from ice melting *in situ*. The height of the **PL** terrace at **a**. is ~4400 m asl, and b., ~4370 m asl and the valley floor in front of the debris-covered glacier ~4330 m asl. A glacier margin at the higher level is commensurate with the tongue extending to the rock step at Franc's Camp (Figure 2,3).

Presence of permafrost?

Feature mapping shows that glaciers play a major role in producing the features seen. The study area showed no indications of permafrost. The Shoshgal valley floor (**VF**, Figure 6(b)) is a low-

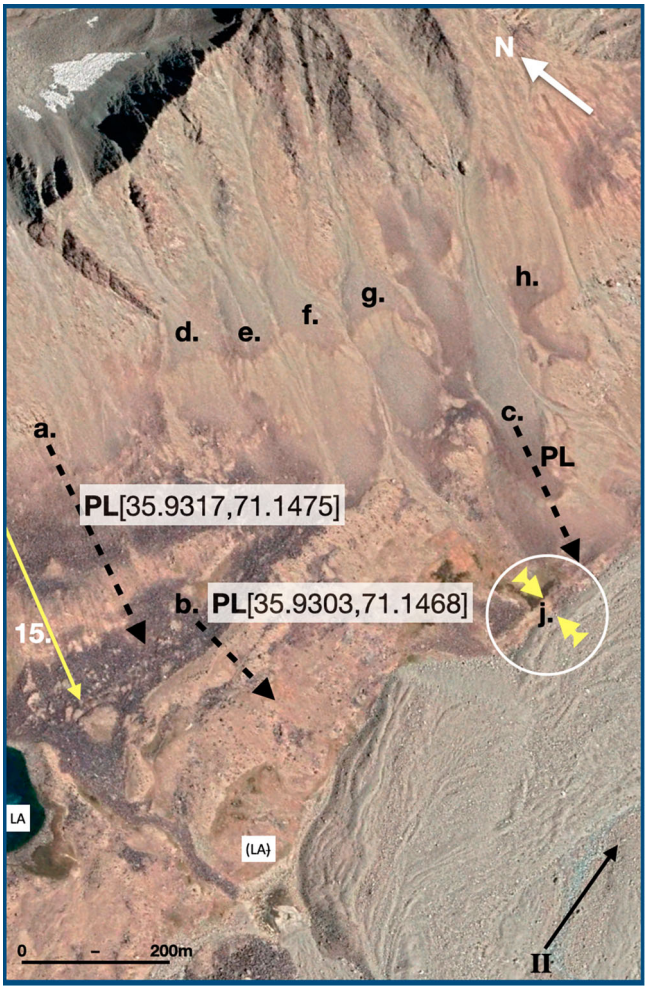

Figure 12. Detail of the lower part of the slop topography near transect 15. Centre of the GE image is [35.9288,71.1471]. The lateral snout of debris-covered glacier of profile II, location of once ice-dammed lake (~~LA~~)[35.9274,71.1440] (Figure 10). Protalus lobes, **PL**, and features a – h are discussed in the text. Some 500 m left, west, of the lake at about [35.9307,71.1370] is a complex of (mostly dark-coloured) features that may be left-lateral moraines (~4580 m asl) of the glacier lobe that was in the basin now containing the lake. This complex is not explored further here. Image ©Google Earth.

angle meadow with thin silty soils and outwash with small pools and summer grazing. The presence of small retreat moraines (**MT** 1 and 2 Figure 6(b)) show that the composite valley glacier system once extended this far. However, no signs of hummocks or thufur were seen in 1976 that might indicate seasonally frozen ground. This meadow is at ~4250 m asl, well below the expected permafrost limit on meteorological grounds. The generalized map of Grötzbach and Rathjens (1969) implies a snowline of ~5200 m asl for the Bashgal area. Their findings suggest that the permafrost zone is likely to be above ~5000 m asl in this area. The enlarging meltwater ponds on glaciers and rock glacier above ~4500 m asl and the permanence of the large pool at [35.9376,71.1525] suggests the permafrost limit is currently well above this altitude.

Valley-side **RG** or **PL** might indicate permafrost, especially when showing flow features. In the study area **PL** have been mapped at various locations on the upper valley sides, at ~4300 m asl [35.9264,71.1577] ~4450 m asl [35.9314,71.1472] on the south facing slopes of the Shoshgal (Figures 11 and 12). A 'down-wasting glacier' model accounts for the north-facing **PL** features of transects 11. 14. and a glacier ice lobe in the side basin accounts for the lower **PL** terraces (15,& a.b.). Thus, **PL**

features are glacial or near glacial accumulations of weathered slope debris and are not permafrost-related. If they had been under permafrost conditions **PL** would be expected (under the permafrost model) to accrete ice and deform over time. Azizi and Whalley (1995, 1996) and Whalley and Azizi (2003) have shown on rheological grounds that flow of rock-ice mixture cores are unlikely. The **PL** described above are relatively old (mid-brown) and pre-LIA, certainly the age of the glacier tongues below. Being at high altitude and with winter snow there seems to be no likelihood of permafrost generation leading to creep. This has also been shown for rock glaciers in Iceland (Whalley 2021b), a relatively maritime climate and the dry Mediterranean Pyrenees (Whalley 2021c). In all cases, the features mapped can be explained by relative movements of weathered rock debris and snow and ice and the flow of glaciers and their protection by debris loads. We can conclude that all these lines of evidence do not indicate permafrost conditions in the recent past in the Upper Bashgal 𝕃𝔻.

Summary of analysis and discussion

The high mountain features in the study area are of two main types; rock-related and ice-related. Bare rock cliffs (**FF**) supply weathered debris to scree slopes (**SS**) and snow and ice supply glaciers (**GL**). The landsystem mapping approach examines how these interact to produce a range of features, particularly **RG** and **MT/ML**. The observations can be linked, allowing a summary of landsystem findings.

Upper mountain system and trunk valleys (with selected examples)

(1) Glaciers and snowfield on steep rock mountain faces and ridges (**AR**) from ~5000 m asl. Weathered rock debris falling from faces to trunk valley glacier surfaces as rockfall and slush/avalanches in spring. Debris incorporated into glacier in accumulation area: ***↓FF/BR↠GL***[35.9497,71.1157] and ***↓FF/BR↠SS↠GL***[35.9463,71.1014].

(2) Glaciers with no surface debris at snouts are rare [35.8766,71.1330]; usually the sequence is: ***GL↠GLd*** or ***GL↠GLd↠RG***

(3) The present glacier/rock glacier shows limits (indicated by light grey surfaces on snout/fronts), there (generally) are no moraines or lateral moraines in the terminal area (unlike major glaciers in the Alps and eastern Himalaya): ***GL↠GLd***| (~~MT,~~ ~~ML~~) or ***GL↠GLd↠RG***| (~~MT~~).

(4) Tributary glaciers largely debris-free in upper reaches glaciers and where their accumulation area is substantial [35.935,71.097], ~5400 m asl reach low altitudes [35.9261,71.1244] ~4750 m,

(5) Some tributary rock glaciers have melt ponds, **RG.p**[35.9108,71.1685] ~4490 m asl, apparently developed 1976–2019, especially in upper and middle reaches: ***GL↠GLd↠RGp*** these glaciers are often associated with exposed surface ice cliffs (**.i**) as at **GLd**[35.9108,71.1667].

(6) Rock glaciers [35.9221,71.1599] ~4150 m asl and main glaciers with heavy debris covers [35.9228,71.1568] ~4150 m asl have 'advancing' snouts with steep, loose fronts. One advancing over (older) terminal moraine sequence on the valley floor [35.9221,71.1599].

(7) A glacier with a heavy debris load has steep lateral moraines between which the glacier has lowered, [35.9253,71.1399] to [35.9218,71.1411] and been restricted.

(8) Lateral scree slopes in lower valleys [35.9326,71.1722] are distinct from glaciers and rock glaciers and show no sign of flow structures, and at high altitudes with dark brown surfaces show considerable age [35.9375,71.1442].

(9) Some scree slopes, particularly on south-facing slopes, have benches [35.9322,71.1466], classed here as **PL**, show no flow structures and bear similar forms to kame terraces/moraines.

(10) Away from the main glaciers there are high altitude small snowpatches that may have protalus rampart features, **PR**[35.9388,71.1388].

High altitude side valley (cirque) systems

(1) Most side (cirque) valleys have bare glacier ice below steep and extensive rock wall free faces feeding debris to glacier systems: ↓***FF/BR***↠***GL***[35.9027,71.1465] thence to rock glaciers ↠***GL***↠***RG***.
(2) Glaciers free from surface debris to the snout are rare, except at high altitude, ***GL***⇢| [35.9070,71.1344], more usually ***GLd*** ⇢ ***MT***[35.9187,71.1360].
(3) Most glaciers have debris-covered fronts ***GL***↠***GLd*** perhaps with **MT** [35.8683,71.1348] or become rock glaciers ***GL***↠***GLd***↠***RG***[35.8707,71.1375].
(4) Cirque glaciers show down-wasting in their upper regions, indicated by meltwater ponds (**.p**) or ice cliff exposures (**.i**), especially where there is little debris cover: **GLp.**[35.8651,71.1762]. Note that a 4000 m^2 area at [35.8703,71.1385] appears to be a now drained pond in **GLd**.

Lower valley slopes, trunk and side valleys

These valleys and slopes are generally below the glaciers or above the glaciers on high, non-glacierized valley sides.

(1) Bare rock outcrops **BR** deliver debris to **SS**, **BR**↠**SS** down to valley floors [35.9326,71.1722].
(2) Avalanching in spring brings down debris to lower slopes, **SS**↠**VF**
(3) Rockfalls/rockslides occur but mainly as old, dark-varnished, deposits [35.9231,71.1588].
(4) Debris may be removed down valley axes with floods **VF**⇝.

Findings and summary images

Figures 13 and 14 provide summary illustrations of the main findings. Figure 13 shows mainly north-facing slopes with substantial **GL**, **GLd** and **RG** components whereas Figure 14 is representative of south-facing slopes

In Figure 13(c) note that:

(i) Interpretation of present-day features from a. and b. Distances show approximate ground lengths taken from GE. The operators indicate, conjectural, relative importance, via arrow length, of debris and ice inputs into various parts of the system.
(ii) Interpretation of earlier advance from the evidence presented in this paper and the over-running of **MT** by **RG**. Low input of debris to the glacier system.

There is no evidence that permafrost-produced flow features exist in $\mathbb{Dm}$ and that glacier ice can produce *all* the features **RG, MT, ML** seen. Specifically, we find relationships:

(i) That **GL** ice must go *somewhere* when it disappears under **GLd**
(ii) That **.p** and **.i** features can be seen in **GLd** and **RG** components, revealing glacier ice.
(iii) That the predominance of **RG** occur increasingly down-valley as a consequence of increased debris load compared with glacier transport effectiveness
(iv) Some moraines were evidently formed by pre- or very early LIA glaciers
(v) As glaciers decayed, post LIA maximum, **FF** area increased, thereby increasing the debris flux to the glacier transport system
(vi) Surficial load on the buried glacier is very effective in preserving glacier ice cores.
(vii) The glacier snouts in the main valleys appear to be advancing because of this protection.
(viii) It is difficult to see how ice-rock mixtures form in the 'rooting zone' = **GLd**, this is an area of glacier down-wasting under a relatively thin surface debris cover.

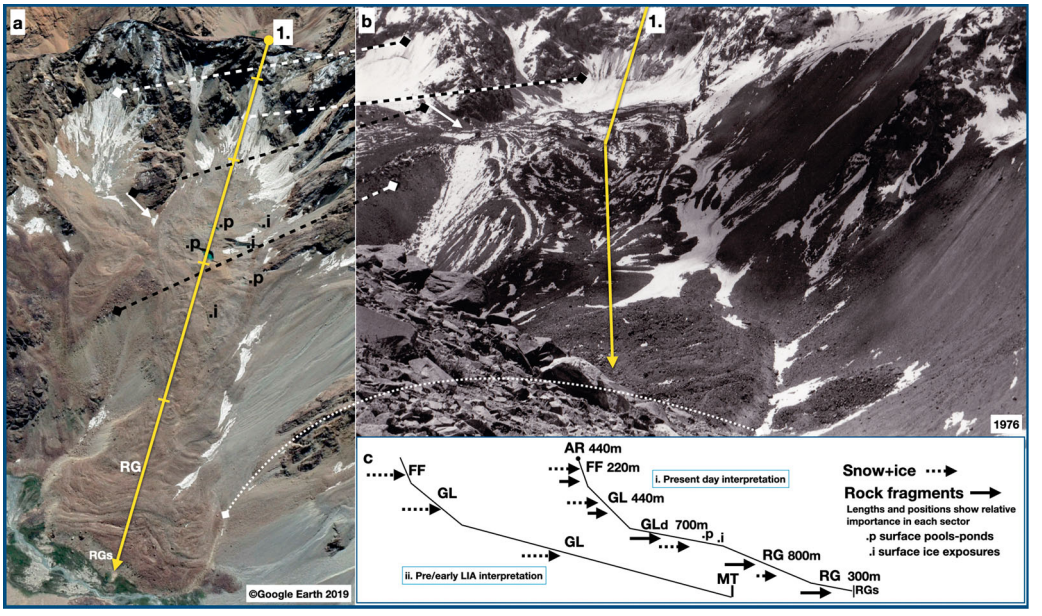

Figure 13. Summary of mapping and information tensors related to the study area, north-facing slopes, and transect 1. [35.9033,71.1720],332. Dashed lines in a and b show corresponding locations in the images. The transects show input and transfers of ice and debris to the resultant landforms. (a) Google Earth Image 2019. Oblique view with transect 1. shown. ©Google Earth. (b) 1976 image taken early summer with corresponding features to a. Note that the section **GLd** is foreshortened. The upper glacier/snowfield **GL** shows debris transported by slush avalanches. Image ©W. Brian Whalley CC BY 4.0. (c) Information tensor approach to summarizing transect 1.; feature digraphs as in Table 1. Note that **RG** in the lower section with surface furrows as in a. but probably advancing snout **RGS**. Image ©W.Brian Whalley CC BY-SA 4.0 2024.

(ix) Studies show that the flow rate of ice-rock mixtures, even if 'super-saturated' with ice, is *much less* than observed **RG** flow rates

(x) Debris slopes, **SS**, show no flow features, as might be expected if meltwater can freeze and accumulate in pore spaces.

(xi) If permafrost can form in a high mountain environment it must be local temperature driven. The long south-facing slopes (such as transect 15) have no glaciers but there are no signs of 'permafrost flow' even at the very highest altitudes. These slopes have been stable over time as illustrated by the varnish colouration.

(xii) Transects from high to lower altitudes (5. – 1.) show progressively, the predominance of glacier ice over debris supply to predominance of debris supply over glacier ice supply. These are also time related, 'youngest' to 'oldest' (5. – 1.).

No evidence for 'permafrost rock glaciers' was found; this negates the mapping of permafrost and inventory by Schmid et al. (2015) and shows the importance of good ground truth investigations.

This area of the Hindu Kush shows true glaciers, usually with heavy debris cover in their lower reaches (~4000 m asl). Most valley glaciers, with debris-free accumulation areas, rapidly accrue heavy surface debris loads and are essentially rock glaciers with snouts about 4500 m asl. This 'conversion' to rock glaciers is attributed to an 'excess' debris supply on top of receding glaciers. Some tributary glacier–rock glaciers systems are shorter in length but steeper than the main trunk glaciers and may be advancing over valley floors. All rock glaciers can be explained as glaciers with debris loads. The insulation provided by heavy debris loads allows ice preservation and descent to lower altitudes than if there was no debris cover. Although the permafrost level is in the region of 5000 m asl. (Grötzbach and Rathjens 1969), there are no landforms which are unequivocally associated with such a thermal regime below or even above this level (Figure 14). All rock glaciers are found well

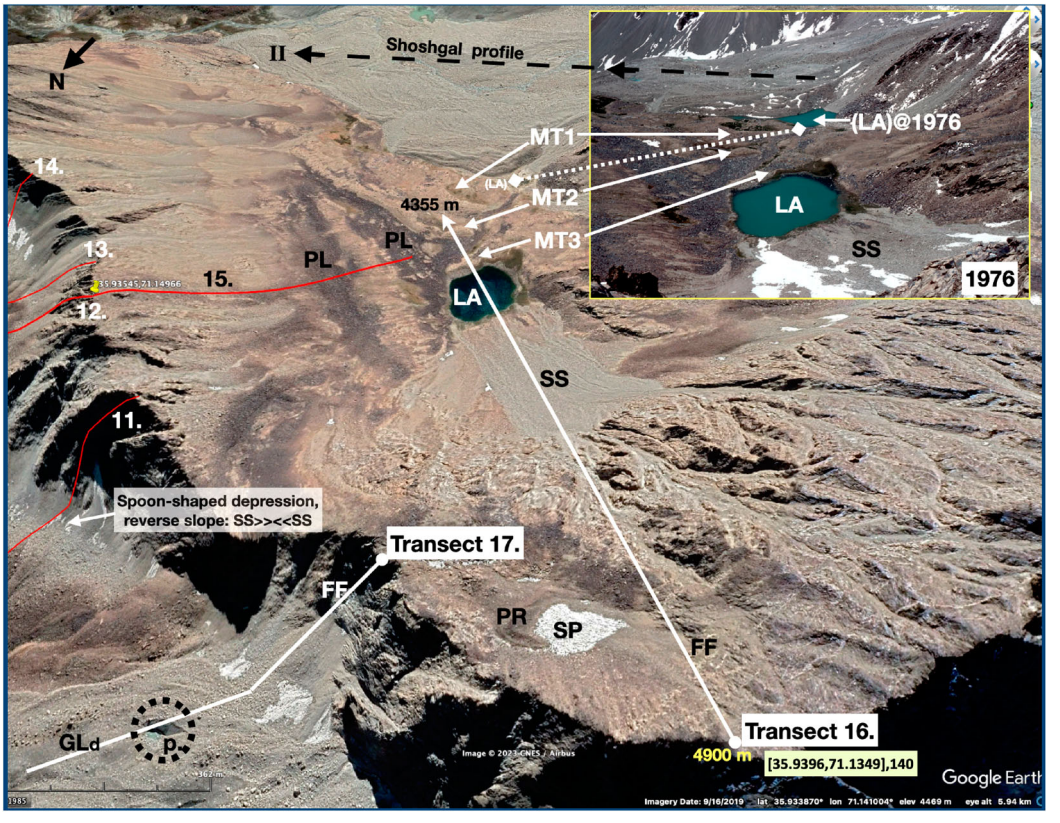

Figure 14. Oblique GE 2019 perspective of south facing slope looking southwest towards the Shoshgal profile (II) with, inset, a terrestrial, 1976, view from about the start of transect 16. Moraines (**MT1**, **2 3**) beyond the main lake were identified in the field and then located in GE. No rock glaciers were found; compare north-facing glacier debris (**GLd**) system of transect 17. and surface pond, **p.**[35.9409,71.1443] and ice cliff. Relative ages are indicated by surface colouration. Image location and direction [35.9396,71.1349],140. Image ©Google Earth. Inset ©W.Brian Whalley BY-SA 4.0 2024.

below 5000 m asl, snouts at 4000–4500 m asl are typical. No examples of rock glacier being derived directly from the copious scree deposits of the area have been seen, nor are they derived from any large Little Ice Age moraines visible in the high corries at ca. 5000 m asl.

In summary, for north-facing slopes glacial conditions predominate (Figure 13) and debris transport is on top of glacier ice producing **GLd** and/or **RG**. Glaciers are at least early LIA being precipitation-temperature controlled. Weathered material from **FF** accumulates as **SS** with little subsequent movement. On south facing slopes, (Figure 14) positive temperature control is predominant with little present glacier cover and debris transport. **SS** are stable and no flow features are present.

Discussion

Mapped features in the $\mathbb{Dm}$ provide a basis for comparing distinct areas when used with cited dLL geolocations. Mapped landforms help construct an information surface using a range of landforms and their interactions rather than relying on a single feature interpretation. Zhou et al. (2022) discussed a deglaciated foreland of the Aerzailaikunai glaciers in the eastern Tienshan [L14]. Topographically, and perhaps climatically, this is similar to the present field area. They suggested that;

> 'under the *periglacial climate* (a) and *thick debris covers (b)*, *ice-rich moraines* are preserved in deglaciating forefields (c), and some of them move downslope by *viscous creeping* (d) and form some characteristics of *rock glaciers* (e)'.

Monnier et al. (2014) examined rock glacier–debris-covered glaciers and assume a permafrost model in a 'periglacial climate' or 'periglacial environment'. Confusingly, 'periglacial' is taken to imply 'permafrost' (Millar and Westfall 2008) as it can also mean 'non-glacial'. Haeberli (1985) considered the Gruben rock glacier [L2] as 'creeping permafrost' (Gärtner-Roer et al. 2021 2024) despite a glacigenic land system explanation (Whalley 2020).

Transect mapping shows how weathered debris is moved downhill, although, as yet, it is difficult to quantify volumes moved over the course of 'deglaciation', post LIA. Screes can build up gradually and some continue to do so (using colour-surface comparisons) but material is also moved directly to glacier surfaces as a debris load. Rockfalls (**RF**) may have been more common than mapped but rockfall debris has probably been incorporated into glaciers/rock glaciers. Future quantification should be possible using a suitable DEM with geo-referenced locations and areas.

In the upper basins of most contributing glaciers, debris cover thickens downslope to produce debris-covered glaciers then becoming rock glaciers. Lateral moraines, **ML**, as distinct topographic features *beyond* present-day snouts were not found. Terminal moraines (**MT**) are either at high altitude terminations of currently active glaciers or on the valley floor as recession moraine ridges. These effects appear to be related to the balances between debris supply to glaciers and subsequent transport.

The valleys are all 'deglaciating' but debris cover protects glaciers from melting as it progressively thickens. This insulation seems particularly effective in the HK where high air temperatures, dry continental conditions and high altitude promote sublimation. Summer snow and wetting of surface debris seem to be rare in these non-monsoonal conditions. However, the last 40 years have seen melt ponds, **.p**, develop on many debris-covered glaciers and rock glaciers and is increasingly common in the 'dry Andes' (Whalley 2023b). The development of melt ponds is shown to be widespread on **RG** and **GLd** in the study area, even at high altitudes.

Tensor information about profiles, e.g. **GL:RG**[35.9033,71.1720]:[35.9228,71.1596] indicates that this is a glacier-rock glacier sequence starting at the [dLL] specified location and terminating at the coupled dLL position.

The transects used in this analysis provide a useful way of plotting future topographic changes (Table 4). With start points given by a [dLL] and a direction they provide survey lines for UAV surveys with various sensors. Coupled with high-resolution satellite imagery, transect data allows repeat surveys to be made and to plot changes over time. This would be a more economic and practical way to use imagery, direct volume changes for example, rather than systems that only recognize shapes of glacier or rock glaciers to produce area averages from inventories. Glacier mass balances could be estimated this way and linked to meteorological conditions that might reflect winter storm or monsoon paths as well as functional changes in geomorphic information tensors (Whalley 2021a). Examining ***→GL→ML/MT*** transport systems in relation to [dLL]-identified glaciers might show behaviour under different climate conditions (Deswal et al. 2023; L18). The tensor

Table 4. Illustration of how geo-locate profiles/transects might be used to show how long-term changes in disposition of features could be monitored. Three profiles are shown here but a fuller compilation might be used for area comparisons over time.

Transct	Start dLL	Start bearing	Altitude m	(Approx.) End dLL	End Altitude m	Height difference	Length (horiz) km	Description
1	[35.9033,71.1720]	332	4975	[35.9228,71.1596]	4130	845	1.36	GL:RG advancing to valley floor, north-facing
3	[35.9030,71.1389]	033	5150	[35.9204,71.1516]	4230	920	2.22	GL:RG
II a	[35.9174,71.0964]	074	5430	[35.9253,71.1319]	4650	780	3.25	Main valley, upper portion
II b	[35.9253,71.1319]	096	4650	[35.9233,71.1567]	4185	465	2.24	Main valley, lower portion

approach should also be capable of linking to methods of mountain hillslope data collection (Clubb et al. 2022) and model interpretation (Brierley et al. 2021).

'Viscous creep', has been used to promote the 'permafrost' rock glacier model (Haeberli 1985; Haeberli et al. 2023), but disputed by modelling (Whalley and Azizi 2003). Ice creeps as a non-Newtonian solid (NB 'viscous creep' can be Newtonian) and is how glaciers flow (as opposed to slide). The Gruben rock glacier [L2] site (Whalley 2020) shows clearly that a debris-covered glacier *does* become a rock glacier. Thin glaciers (< ~50 m thick) at low surface slope angles (< ~10°) have surface measured velocities generally <~1 m/a, that of most rock glaciers. As surface lowering takes place (as on the profile a-b on II) the glacier will slow, if it continues to advance it will also thin and slow. The characteristic of debris-covered glaciers becoming rock glaciers (defined as topographic forms) is seen in nearly all the examples in the study area; rock glaciers are advancing over the valley floor as the ablation area is protected; ***FF:GL:GLd:RG*|VF,** and explains all visible topographic forms and is common in the main valleys of the $\mathbb{Dm}$ landsystem.

The 'permafrost inclusive – glacier ice exclusive' notion for rock glaciers assumed by, amongst others, Brardinoni et al. (2019), RGIK (2022), Schmid et al. (2015) follow Barsch (1996, p. 208) who says, 'rock glaciers, debris covered glaciers and (ice) glaciers are found in the same neighbourhood' and that this is an 'areal, not genetic connection'. However, this paper finds that there *is* a genetic link in the development of rock glaciers from glaciers where there is sufficient insulating supraglacial cover. Kinzl (1932) was correct in his assertion that **RG** 'are nothing other than the preserved glaciers of the last [19th] century' (Barsch 1996, p. 208).

Munroe (2018, p. 51) has suggested, 'ice-cored and ice-cemented rock glaciers likely inhabit opposite ends of a continuum of related landforms' but that (p. 59) 'An unsolved question in rock glacier research is what controls the presence or absence of rock glaciers'. The present study shows that there is *no* such continuum of landforms rather, that glacier flow *continuum mechanics* adapts to varying debris and ice inputs to mountain slopes. This paper shows that there is no reason to believe that permafrost-produced ice-rock mixtures give rise to rock glaciers. There is no evidence for 'permafrost rock glaciers' and no need to invoke this origin. Glacier ice with a protecting debris load is sufficient to explain *all* the features seen and is a parsimonious model.

The listed landform/process relationships provide an integrated means of establishing connectivity criteria for identification and monitoring of high $\mathbb{Dm}$ environments and change that might be used in machine learning procedures, and probabilistic mapping (Kirkwood 2022) rather than relying on a few visual entities (Hu et al. 2023).

Conclusions and future work

This paper shows that the landsystem approach to mapping and recording significant geomorphological features in a specific $\mathbb{Dm}$ offers advantages over 'static' mapping and description of individual landforms. The use of Google Earth coupled to specific feature and place location by [dLL] greatly enhances field observations and features that can be recorded directly on GE images and extend the idea of the Digital Earth (Gore 1999). Transect mapping allows examination of debris transfer relationships between slope elements allowing comparisons between areas. In the area considered, all landforms are consistent with a glacier-dependent model. Specified and published [dLL] location increases the value of geomorphological contributions by conforming to the FAIR data principles allowing, for example better inter-site comparisons (Whalley 2024).

The main landforms examined in 1976 and compared to 2019 GE imagery shows they are *all,* **RG** and **GLd**, being related to flux balances of glacier ice and weathered rock debris onto glaciers. The LIA produced mainly debris-covered glaciers and rock glacier-like snouts that became the glacial (i.e moraine) limits over time. This is seen in examples in the study area (Figure 9).

All the debris-derived landforms in these valleys can be related to either scree formation or in debris-ice continua of varying activity. Recent (50 year) ice ablation, especially in the upper reaches

of the glaciers, shows the development of surface melt ponds in **GLd** and **RG**. These melt ponds are less common in the lower reaches of the debris-covered glaciers and rock glaciers as melting is limited by increasing debris thicknesses. Nevertheless, in the long term, melt ponds should increase in size and frequency downstream. Some predictions can be made:

(i) despite general glacier retreat, some rock glaciers and heavily debris-covered glaciers may show continued advances and debris slumps at rock glacier snouts may eventually reveal glacier ice cores.
(ii) melt ponds are likely to be found increasingly in the lower portions of some rock glaciers as well as debris-covered glaciers and link to ice exposures at snouts. Pond sizes will increase.
(iii) reverse scree slopes (**SS><SS**) (transect 11.) will become more extensive downslope as the ice melts. These concavities are not permafrost rock glacier 'rooting zones' but 'spoon-shaped hollows' (Outcalt and Benedict 1965; Whalley and Azizi 2003) reflecting the restricted surface melting of debris-covered glaciers.

Using the dLL specifications as suggested above would allow a variety of questions to be answered in addition to the three just posed.

No evidence of permafrost has been found. This is contrary to the suggestion of Schmid et al. (2015, *supra*), that rock glaciers are '*visual indicators of permafrost*, [they] can occur near the *lowermost regional occurrence of permafrost in mountains*' Schmid et al. (2015, p. 2089). That rock glaciers are caused by mountain permafrost is confirmation bias (Jones and Sugden 2001; Brierley et al. 2021) following statements by Barsch (1987, 1996). Further, that rock glaciers indicate permafrost has been falsified for many years and further in this paper. The 'permafrost rock glacier' statements by Schmid et al. (2015) and Monnier and Kinnard (2017) are incorrect. A continuum or transition from ice-cored to ice-cemented rock glaciers does not exist, nor are rock glaciers 'equifinal' landforms (Knight et al. 2019). All statements about permafrost in the mountain domain, past or present, being indicated by 'rock glaciers' should be re-evaluated and deprecated in future.

This paper has brought together observations on the topography, glacier and rock debris locations and movements in a specified landsystem; a high mountain landscape domain, $\mathbb{Dm}$. Work in progress exploits such [dLL] geolocation within this common co-ordinate system that avoids the 'uniqueness' of much geomorphological reporting. Observed events reported in the literature can be brought together as geomorphic information fields considered via 'events' in geomorphological spacetime diagrams. To these fields, meteorological and climatological information can be added as well as extending the range of glacio-debris mass balance changes across the Hindu Kush-Karakorum.

Acknowledgements

I thank John Gordon and Martin Gledhill for their comments on a draft of this paper and to those of two reviewers. The fieldwork presented here was carried out on the 1976 Cambridge Hindu Kush Expedition and I thank the members for their assistance throughout the expedition: Chris Hore, Roger Aylard, Tim Hurrell, Martin Gledhill, Francine Hughes, Joy Richardson and Deborah Wells. Collectively, we would like to thank our sponsors especially awards by the 20th International Geographical Congress Fund and the Mount Everest Foundation. We also thank the Afghanistan and UK authorities in both London and Kabul in 1975–1976 and, not least, remember the invaluable help and comradeship of Noor Mohammed and Abdul Ghani of Nuristan. This paper is dedicated to them and the late Tim Hurrel killed on Kuksar in the Karakorum, Hal Lister, pioneer glacier meteorologist and explorer and the late Peter Birkeland, Quaternary landform explorer.

Disclosure statement

No potential conflict of interest was reported by the author(s).

Notes on contributor

W. Brian Whalley retired from Queens University Belfast and now lives in Sheffield, Yorkshire, where he is Emeritus Honorary Professor in the Department of Geography in the University of Sheffield. He continues to work on glacial geomorphological problems and geoheritage but also researches in education, particularly related to fieldwork and mobile technologies. He is an Honorary Life Member of the British Society for Geomorphology and a National Teaching Fellow.

Location list

This list provides locations of examples and comparison sites not in the study area but designated by [dLL] in sequence as mentioned in the text. It is a location companion to the references cited. Note that the reference to the literature given may not be the only linkage to a given feature.

L1 [44.6431,−109.7916] Galena Creek rock glacier, WY, USA. (Potter 1972)
L2 [46.1740,7.9669] Gruben rock glacier, Switzerland. (Whalley 2020)
L3 [65.4917, −18.3686] Nautardalur rock glacier, Iceland. (Whalley 2021b)
L4 [42.6578,0.4448] Posets glacier and rock glacier, Pyrenees. (Whalley 2021c)
L5 [34.1194,75.5045] Wavbal Pass, Jammu and Kashmir. (Mayewski et al. 1981)
L6 [35.5910,70.1642] Mir Samir, Afghanistan. (Gilbert et al. 1969)
L7 [35.5877,72.9641] Glacier within distinct lateral moraine arcs, Kohistan.
L8 [46.0562,7.9438] Findelengletscher, Switzerland
L9 [−30.1579,−69.9209] complex **GL:RG** system, Andes (Monnier and Kinnard 2017)
L10 [46.1008,7.9120] Feegletscher moraines, Switzerland. (Whalley et al. 1996)
L11 [69.7030,20.2088] Strupbreen, N Norway. (Whalley 1976)
L12 [44.5554,6.8622] Marinet rock glacier, France. (Whalley and Palmer 1998)
L13 [57.073,−2.889]. Kame terraces, Muir of Dinnet, Scotland. (Gordon 1993)
L14 [43.314,85.073] Aerzailaikunai glaciers, Tienshan. (Zhou et al. 2022)
L15 [−30.1695,−69.9281] Dry Andes. (Monnier and Kinnard 2017)
L16 [−32.8878,−70.0413] Dry Andes. (Monnier and Kinnard 2017)
L17 [−32.8878,−70.0413] Dry Andes. (Monnier and Kinnard 2017)
L18 [32.7737,76.9266] Neelkanth Glacier. (Deswal et al. 2022)

ORCID

W. Brian Whalley http://orcid.org/0000-0003-3361-3527

References

Azizi F, Whalley WB. 1995. Finite element analysis of the creep of debris containing thin ice bodies. The Fifth International Offshore and Polar Engineering Conference. The Hague: International Society of Offshore and Polar Engineers; p. 336–342.

Azizi F, Whalley WB. 1996. Numerical modelling of the creep behaviour of ice-debris mixtures under variable thermal regimes. The Sixth International Offshore and Polar Engineering Conference. International Society of Offshore and Polar Engineers. ISOPE-1-96-138.

Baraka S, Akera B, Aryal B, Sherpa T, Shresta F, Ortiz A, Sankaran K, Ferres JL, Matin M, Bengio Y. 2020. Machine Learning for Glacier Monitoring in the Hindu Kush Himalaya. arXiv preprint arXiv:2012.05013.

Baral P, Haq MA. 2020. Spatial prediction of permafrost occurrence in Sikkim Himalayas using logistic regression, random forests, support vector machines and neural networks. Geomorphology. 371:107331. doi:10.1016/j.geomorph.2020.107331.

Barsch D. 1987. The problem of ice-cored rock glacier. In: Giardono JR, Shroder JF, Vitek JD, editor. Rock glaciers. London: Allen and Unwin; p. 45–53.

Barsch D. 1992. Permafrost creep and rockglaciers. Perm Periglac Process. 3(3):175–188.

Barsch D. 1996. Rockglaciers. Indicators for the present and former geoecology in high mountain environments. Berlin: Springer.

Blöthe JH, Rosenwinkel S, Höser T, Korup O. 2019. Rock-glacier dams in high Asia. Earth Surf Proc Landf. 44 (3):808–824.
Bolch T, Shea JM, Liu S, Azam FM, Gao Y, Gruber S, Immerzeel WW, Kulkarni A, Li H, Tahir AA. 2019. Status and change of the cryosphere in the extended Hindu Kush Himalaya region. In: Wester P., Mishra A., Mukherji A., Shrestha AB, editors. The Hindu Kush Himalaya assessment: mountains, climate change, sustainability and people. Cham: Springer; p. 209–255.
Bowlby SR, White KH. 2019. The geographical background. In: Allchin R., Hammond N., Ball W, editor. The archaeology of Afghanistan, from the earliest times to the Timurid period (new edition). Edinburgh: Edinburgh University Press; p. 15–60.
Brardinoni F, Scotti R, Sailer R, Mair V. 2019. Evaluating sources of uncertainty and variability in rock glacier inventories. Earth Surf Proc Landf. 44(12):2450–2466.
Brierley G, Fryirs K, Reid H, Williams R. 2021. The dark art of interpretation in geomorphology. Geomorphology. 390:1–13 j.geomorph.2021.107870.
Brunsden D, Thornes J. 1979. Landscape sensitivity and change. Trans Inst Br Geogr. 4(4):463–484. doi:10.2307/622210.
Chakravarti P, Jain V, Mishra V. 2022. The distribution and hydrological significance of intact rock glaciers in the north-west Himalaya. Geogr Ann A. 104(3):226–244.
Chandler R. 1973. The inclination of talus, Arctic talus terraces, and other slopes composed of granular materials. J Geol. 81(1):1–14.
Clubb FJ, Weir EF, Mudd SM. 2022. Continuous measurements of valley floor width in mountainous landscapes. Earth Surface Dyn. 10(3):437–456. doi:10.5194/esurf-10-437-2022.
Deswal S, Sharma MC, Saini R, Chand P, Prakash S, Kumar P, Barr ID, Latief SU, Dalal P, Bahuguna I. 2023. Reconstruction of post-little ice age glacier recession in the Lahaul Himalaya, north-west India. Geogr Ann A Phys Geogr. 105(1):1–26. doi:10.1080/04353676.2022.2148082.
Evans DJ. 1993. High-latitude rock glaciers: a case study of forms and processes in the Canadian arctic. Perm Periglac Process. 4(1):17–35.
Evans DJA. 2003. Glacial landsystems. London: Hodder.
Gabet EJ. 2003. Sediment transport by dry ravel. J Geophys Res Solid Earth. 108(B1):22-1–22-8.
Gärtner-Roer I, Brunner N, Delaloye R, Haeberli W, Kääb A, Thee P. 2021. Glacier-permafrost relations in a high-mountain environment: 5 decades of kinematic monitoring at the Gruben site, Swiss Alps. Cryosphere Disc. 1–30. https://doi.org/10.5194/tc-2021-208.
Gilbert O, Jamieson D, Lister H, Pendlington A. 1969. Regime of an Afghan glacier. J Glaciol. 8(52):51–65.
Gordon JE. 1993. Muir of Dinnet. In: Gordon JE, Sutherland DG., editor. Quaternary of Scotland. London: Chapman and Hall; p. 246–251.
Gore A. 1999. The Digital Earth: understanding our planet in the 21st century. Australian Surveyor. 43:89–91.
Grötzbach E. 1965. Beobachtungen an Blockströmen im afghanischen Hindukusch und in den Ostalpen. Mit der Geogr Ges München. 50:175–201.
Grötzbach E, Rathjens C. 1969. Die heutige und die jungpleistozäne Vergletscherung des afghanischen Hindukusch. Zeit für Geomorphol. Supp. 8:58–75.
Grove JM, Switsur R. 1994. Glacial geological evidence for the medieval warm period. In: Hughes MK, Diaz HF, editor. The medieval warm period. Amsterdam: Kluwer; p. 143–169.
Haeberli W. 1985. Creep of mountain permafrost: internal structure and flow of alpine rock glaciers. Mit Ver Was Hydrol Glaziol. 77:142.
Haeberli W, Arenson L U, Wee J, Hauck C, Mölg N. 2023. Discriminating viscous creep features (rock glaciers) in mountain permafrost from debris-covered glaciers–a commented test at the Gruben and Yerba Loca sites, Swiss Alps and Chilean Andes. EGUsphere. 2023:1–23.
Hu Y, Liu L, Huang L, Zhao L, Wu T, Wang X, Cai J. 2023. Mapping and characterizing rock glaciers in the arid west Kunlun mountains supported by InSAR and deep learning. Journal Geophysical Research: Earth Science. doi:10.1029/2023JF007206.
Janke J, Regmi NR, Giardino JR, Vitek JD. 2013. Rock glaciers. 8.17 Treatise on Geomorphology. Amsterdam: Elsevier; p. 238–273.
Jones D, Harrison S, Anderson K, Selley H, Wood J, Betts R. 2018. The distribution and hydrological significance of rock glaciers in the Nepalese Himalaya. Global Plan Change. 160:123–142. doi:10.1016/j.gloplacha.2017.11.005.
Jones DB, Harrison S, Anderson K, Whalley WB. 2019. Rock glaciers and mountain hydrology: A review. Earth-Sci Revs. 193:66–90. doi:10.1016/j.earscirev.2019.04.001.
Jones M, Sugden R. 2001. Positive confirmation bias in the acquisition of information. Theory Decis. 50(1):59–99.
Joya E, Bromand MT, Murtaza KO, Dar RA. 2021. Current glacier status and ELA changes since the Late Pleistocene in the Hindu Kush Mountains of Afghanistan. Journal of Asian Earth Sci. 219:104897.
Kinzl H. 1932. Die grössten nacheiszeitlichen Gletschervorstösse in den Schweizer Alpen und in der Mont Blanc-Gruppe. Kinzl, H., 1932. Die grössten nacheiszeitlichen Gletschervorstösse in den Schweizer Alpen und in der Mont Blanc-Gruppe. Zeit Gletscherkunde und Glazialgeologie. 20:269–397.

Kirkwood C. 2022. Geological mapping in the age of artificial intelligence. Geoscientist. 32(3):16–23. doi:10.1144/geosci2022-023.
Knight J, Harrison S, Jones DB. 2019. Rock glaciers and the geomorphological evolution of deglacierizing mountains. Geomorphology. 324:14–24.
Lilleøren KS, Etzelmüller B, Rouyet L, Eiken T, Hilbich C. 2022. Transitional rock glaciers at sea-level in northern Norway. Earth Surf Dyn Discuss. 1–29. doi:10.5194/esurf-2022-6.
Madole RF. 1972. Neoglacial facies in the Colorado Front Range. Arct Alp Res. 4(2):119–130.
Maharjan SB, Shrestha F, Azizi F, Joya E, Bajracharya B, Bromand M T, Rahimi M M. 2021. Monitoring of glaciers and glacial lakes in Afghanistan. In: Bajracharya B, Thapa RB, Matin MA, editor. Earth observation science and applications for risk reduction and enhanced resilience in Hindu Kush Himalaya region. Cham: Springer; p. 211–230.
Marcer M, Bodin X, Brenning A, Schoeneich P, Charvet R, Gottardi F. 2017. Permafrost favourability index: spatial modelling in the French Alps using a rock glacier inventory. Front Earth Sci. 5:105.
Martin HE, Whalley WB. 1987. Rock glaciers: part 1: rock glacier morphology: classification and distribution. Prog Phys Geogr. 11(2):260–282.
Mayewski PA, Jeschke PA. 1979. Himalayan and trans-Himalayan glacier fluctuations since AD 1812. Arct Alp Res. 11(3):267–287.
Mayewski PA, Jeschke PA, Ahmad N. 1981. An active rock glacier, Wavbal Pass, Jammu and Kashmir Himalaya, India. J Glaciol. 27(95):201–202.
McRae BH. 2008. Using circuit theory to model connectivity in ecology, evolution, and conservation. Ecology. 89 (10):2712–2724.
Millar CI, Westfall RD. 2008. Rock glaciers and related periglacial landforms in the Sierra Nevada, CA, USA; inventory, distribution and climatic relationships. Quat Int. 188(1):90–104.
Monnier S, Kinnard C. 2017. Pluri-decadal (1955–2014) evolution of glacier–rock glacier transitional landforms in the central Andes of Chile (30–33 S). Earth Surf Dyn. 5(3):493–509.
Monnier S, Kinnard C, Surazakov A, Bossy W. 2014. Geomorphology, internal structure, and successive development of a glacier foreland in the semiarid Chilean Andes (Cerro Tapado, upper Elqui Valley, 30 08′ S., 69 55′ W.). Geomorphology. 207:126–140.
Munroe JS. 2018. Distribution, evidence for internal ice, and possible hydrologic significance of rock glaciers in the Uinta Mountains, Utah, USA. Quat Res. 90(1):50–65.
Outcalt SI, Benedict JB. 1965. Photo-interpretation of two types of rock glacier in the Colorado Front Range, USA. J Glaciol. 5(42):849–856.
Porter SC. 2011. Late Pleistocene glaciation of the Hindu Kush, Afghanistan. In: Ehlers J, Gibbard PL, Hughes PD., editor. Quaternary glaciations – extent and chronology: a closer look. Developments in Quaternary science.15. Amsterdam: Elsevier; p. 863–864.doi:10.1016/B978-0-444-53447-7.00062-3.
Potter N, Steig E, Clark D, Speece M, Clark GT, Updike AB. 1998. Galena Creek rock glacier revisited—New observations on an old controversy. Geogr Ann A. 80(3-4):251–265.
Potter N. 1972. Ice-cored rock glacier, Galena Creek, northern Absaroka Mountains, Wyoming. Geol Soc Am Bull. 83 (10):3025–3058.
Raup BH, Racoviteanu A, Khalsa SJS, Helm C, Armstrong R, Arnaud Y. 2007. The GLIMS geospatial glacier database: a new tool for studying glacier change. Global Plan Change. 56:101–110. doi:10.1016/j.gloplacha.2006.07.018.
RGIK. 2022. IPA Action Group Rock glacier inventories and kinematics. Towards standard guidelines for inventorying rock glaciers: baseline concepts (Version 4.2.2). Available at: https://tinyurl.com/2p9hbd5m.
Richmond GM. 1962. Quaternary stratigraphy of the La Sal Mountains Utah. US Geol Surv Prof Paper. 324:1–135.
Rowley T, Giardino JR, Granados-Aguilar R, Vitek JD. 2015. Periglacial processes and landforms in the critical zone. In: Giardino JF, Houser C., editor. Developments in earth surface processes, V 19. Amsterdam: Elsevier; p. 397–447.
Schmid M-O, Baral P, Gruber S, Shahi S, Shrestha T, Stumm D, Wester P. 2015. Assessment of permafrost distribution maps in the Hindu Kush Himalayan region using rock glaciers mapped in Google Earth. The Cryosphere. 9(6):2089–2099.
Schweizer G. 1970. Der kuh-e-sabalan (Nordwestiran). Beitrage zur Gletscherkunde and Glazialgeomorphologie vorderasiatischer Hochgebirge. Tübinger Geogr Studien. 34(3):163–178.
Shepherd TG, Boyd E, Calel RA, Chapman SC, Dessai S, Dima-West IM, Fowler HJ, James R, Maraun D, Martius O. 2018. Storylines: an alternative approach to representing uncertainty in physical aspects of climate change. Clim Change. 151(3):555–571.
Sivall TR. 1977. Synoptic-climatological study of the Asian summer monsoon in Afghanistan. Geogr Ann A. 59A(1-2):67–87.
Steig EJ, Clark DH, Potter N. 1998. The geomorphic and climatic significance of rock glaciers. Geogr Ann A. 80A:173–174.
Tranter P. 1968. No Tigers in the Hindu Kush. London: Travel Book Club.

Vishwakarma BD, Ramsankaran R, Azam M, Bolch T, Mandal A, Srivastava S, Kumar P, Sahu R, Navinkumar PJ, Tanniru SR. 2022. Challenges in understanding the variability of the cryosphere in the Himalaya and its impact on the regional water resources. Frontiers in Water. 102:909246. doi:10.3389/frwa.2022.909246.
Wahrhaftig C, Cox A. 1959. Rock glaciers in the Alaska range. Geol Soc Am Bull. 70(4):383–436.
Whalley WB. 1976. A rock glacier and its relation to the mass balance of corrie glaciers, Strupbreen, Troms, Norway. Norsk Geog Tids. 30:52–55.
Whalley WB. 1984. High altitude rock weathering processes. In: Miller KJ, editor. The international Karakoram project. Vol. 1. Cambridge: Cambridge University Press; p. 365–373.
Whalley WB. 2020. Gruben glacier and rock glacier, Wallis, Switzerland: glacier ice exposures and their interpretation. Geogr Ann A. 102(2):141–161.
Whalley WB. 2021a. Mapping small glaciers, rock glaciers and related features in an age of retreating glaciers: using decimal latitude-longitude locations and 'geomorphic information tensors'. Geogr Fis e Dinam Quat. 44(1):55–67. doi:10.4461/GFDQ.2021.44.4.
Whalley WB. 2021b. The glacier – rock glacier mountain landsystem: an example from North Iceland. Geogr Ann A. 104(4):1–22. doi.org/10.1080/04353676.2021.1986304..
Whalley WB. 2021c. Geomorphological information mapping of debris-covered ice landforms using Google Earth: an example from the Pico de Posets, Spanish Pyrenees. Geomorphology. 393:107948. doi:10.1016/j.geomorph.2021.107948.
Whalley WB. 2022. Figures, landscapes and landsystems: digital locations, connectivity and communications. Earth Surf Proc Landf. doi:10.1002/ESP.5418.
Whalley WB. 2023a. Landscape domains and information surfaces: data collection, recording and citation using decimal latitude-longitude geolocation via the FAIR principles. Earth Surf Processes Landforms. 48(11):1–11. DOI: 10.1002/esp.5678.
Whalley WB. 2023b. Comment on "Ice content and interannual water storage changes of an active rock glacier in the dry Andes of Argentina" by Halla, et al. (2021). Plus further discussion and comments. Cryosphere. 17:699–70010.5194/tc-2021-88.
Whalley W.B.. 2024. The geolocation of features on information surfaces and the use of the open and FAIR data principles in the mountain landscape domain and geoheritage. Perm Periglac Process. 1–11. DOI: 10.1002/ppp.2217.
Whalley WB, Azizi F. 2003. Rock glaciers and protalus landforms: analogous forms and ice sources on Earth and Mars. J Geophys Res Planets. 108(E4):13-1–13-17. doi:10.1029/2002JE001864.
Whalley WB, Martin HE. 1992. Rock glaciers: II models and mechanisms. Prog Phys Geogr. 16(2):127–186.
Whalley WB, Martin HE. 1994. Rock glaciers in Tröllaskagi: their origin and climatic significance. Münchener Geogr Arb. 12:289–308.
Whalley WB, Palmer C, Hamilton S, Kitchen D. 1996. Supraglacial debris-transport variability over time: examples from Switzerland and Iceland. Ann Glaciol. 22:181–186.
Whalley WB, Palmer CF. 1998. A glacial interpretation for the origin and formation of the Marinet Rock Glacier, Alpes Maritimes, France. Geogr Ann A. 80(3-4):221–236.
Zhou Y, Li G-Y, Jin H-J, Marchenko SS, Ma W, Du Q-S, Li J-M, Chen D. 2022. Viscous creep of ice-rich permafrost debris in a recently uncovered proglacial area in the Tianshan Mountains, China. Adv Clim Change Res. 13:540–553.